

Dear Prof. McCabe,

We would like to thank you and the two reviewers for their time and excellent comments regarding our manuscript, titled “Feasibility analysis of using inverse modeling for estimating field-scale evapotranspiration in maize and soybean fields from soil water content monitoring networks”. After careful analysis of all the comments, we have made revisions to our manuscript and added a section better explaining the application and limitations associated with the method (3.4). You can find our detailed responses to the reviewers’ comments (shown in red italics) and the changes we made to the manuscript in the following sections. We have also included a marked up version of the original manuscript.

On the behalf of all coauthors, I hope that this revised version would meet the publication standard of Hydrology and Earth System Sciences (HESS) and inclusion in the Eric F. Wood special issue. Please let us know if there are more questions and comments about the manuscript.

Sincerely,

Prof. Trenton E. Franz
School of Natural Resources
University of Nebraska-Lincoln, USA

Reply to the editor:

Thank you for the comments regarding our manuscript. Please see our detailed replies below.

As you will see, I have received two referee report on your revised manuscript. Both appreciate the significant effort that has gone into improving this resubmitted version.

Referee #1 has reiterated a request for some further interpretation of results, ideally in a separate Discussion section. I tend to agree that providing some additional insight into the issues related to your approach, as well as any limitations or advantages, would be useful to the reader. Whether this should be done in a separate Discussion section I will leave to you, but it would be good to see some of your thoughts on the challenges (and opportunities) that may be presented by this approach, as well as addressing the issues raised by Ref #2.

Thank you for the suggestions. We added a separate section (3.4) and explained the applications and limitations of the method in more details.

Referee #2 is largely happy with the changes, but identifies a number of relatively minor corrections in their report. These should be fairly straightforward to address.

Thank you for the comments. We have made the changes as requested.

Overall, I believe the requested changes will not present any major challenges to implement and expect that I will be able to make a final Editorial decision upon receipt of an updated manuscript and a detailed response to the reviewers.

We really appreciate you taking time and reviewing our manuscript. We look forward to hearing back from you about a final decision.

Replies to Anonymous Reviewer #2

Thank you for the comments regarding our manuscript. Please see our detailed replies below.

This is a revised manuscript, and the authors have put in significant effort to address the comments raised in the earlier round of review. As such, the manuscript appears to be vastly improved in terms of comprehensiveness and flow. However, I do have a few minor points that I feel will further improve the manuscript if addressed. I list them below. Apart from this, a further scan for grammar and language would be beneficial. My recommendation to the editor is to

accept the manuscript for publication in HESS subject to the following minor concerns being addressed by the authors.

Thank you for your time and comments. We have modified some of the sentences based on your comments and added a few more details on ET_r calculations for clarity.

Abstract, L27: What is the “plumber experiment”? This is the only location it appears in the manuscript. There is no mention of this experiment in the main text or in the references. If you are mentioning something in the abstract, I would expect it to be materially significant to the narrative, and to read more about it in the introduction section (in this case).

Thank you for the comment. You are right, we never used the term in the manuscript so we just decided to edit the sentence and avoid having the term “plumber experiment” within the abstract.

P5, L89: “... VZM modeling...” Does the M in VZM not stand for model/ing?

Yes, we have deleted the repeated term (L93).

P7, L133: Why was the ET_r computed for alfalfa, and not for either maize (a tall crop itself) or soybean? No justification is provided for using an ET_r from a different crop to the one grown in the particular field. Even if it is a standard procedure to use alfalfa for ET_r , and then use crop coefficients to translate the ET_r for the particular crops, it is necessary to mention that here.

Thank you for your comment. As you mentioned, based on ASCE Penman-Monteith equation (which is a standard procedure), we can just compute reference ET (ET_r) for either grass or alfalfa and then using crop coefficient (K_c) values we can calculate ET_p values for each individual crop. Here we computed ET_r values for alfalfa and then using crop coefficient (K_c) values suggested by Allen et al. (1998) and Min et al. (2015) we calculated ET_p values for maize and soybean. We have tried to make it clearer in the manuscript that we have indeed followed a standard procedure here (L167-169).

L167-169: “Based on ASCE Penman-Monteith equation, ET_r values can be computed for either grass or alfalfa and then using crop-specific coefficients daily potential evapotranspiration (ET_p) can be calculated.”

P7, L143: You mention that the CRNP measurement depth varied between 15 and 40cm, but assume a mean depth of 10cm over the entire period. Why was the mean depth assumed to be outside the 15-40cm range?

Thank you for your comment and sorry for the confusion. The depth varied between 15-40 cm but as we mentioned in the manuscript for simplicity purposes we assumed the CRNP has an effective depth of 20 cm meaning the CRNP soil water content measurement comes from the top 20 cm soil layer. This is a conservative guess for the depth of the sensor. Moreover, we also assign a node at 10 cm for the inverse modeling and estimate of hydraulic properties from a 0 to 20 cm soil depth. This node depth must be assigned in the Hydrus modeling framework.

P11, L225: Contrary to the above point, you mention that the average effective measurement depth was considered to be 20cm, and an observation point was set at 10cm depth. This is confusing.

Please see comment above.

P18, L372: I am happy you bring up the point about equifinality, and thus imply that deterministic modeling may not always be the best option in hydrology. Thank you for discussing this possibility at this juncture.

Thank you for the comment.

Replies to Anonymous Reviewer #3

Thank you for the comments regarding our manuscript. Please see our detailed replies below.

Authors have addressed editor and reviewers' comments in the revised manuscript. Performing sensitivity experiments provided further insights about the modeling results. However, two main issues still remain.

1) While authors report other statistical measures for model performance, they only focused on RMSE values for discussing their results. As shown in Table 3 and raised by reviewer 3 in the first set of comments, it is problematic to have negative NSE values. This means that average observed values are better than model simulation. Authors need to discuss this disagreement.

Thank you for your comment. As it is mentioned in the manuscript RMSE was chosen as the objective function and MAE, NSE, and R^2 are used as the additional evaluation metrics. However, you are right that negative NSE values mean that the simulation results are not as good as mean observed values. We tried to improve NSE values by minimizing the inaccuracy but there are many free parameters involved in modeling that can affect the results. Since we selected RMSE as our objective function (very often done in literature) we felt additional metrics were useful for the reader to gauge the level of goodness-of-fit. If NSE would have been selected

as our objective function you would likely get a different set of parameters. We considered a multi-objective optimization procedure using a compromised solution but thought it was beyond the scope of the current paper. Clearly a weakness in any multiple objective optimization is selection of the objective function(s).

2) As it was raised by the editor and reviewers, a detailed discussion section regarding the limitation and advantages of this modeling study is required. In particular, how combination of CRNP and point measurements of soil moisture observations can be used to provide field scale estimates of E_t .

Thank you for your comment. We added a separate section (3.4) (L427-454).

L427-454: “3.4 Applications and limitations of the vadose zone modeling framework

Given its simplicity and widespread availability of ground data, E_t and K_c values are often used in a wide variety of applications to estimate E_p and thus approximate E_a . It is well known that SWC is a limiting factor affecting the assumption that $E_p \sim E_a$. On the other hand, we know that SWC observations are local in nature and not necessarily representative of E_a footprint estimates. The key questions are: what is the value of SWC observations, how many profiles do we need to install in a footprint, and at which depths to constrain estimates of fluxes? The well instrumented and long-term study presented here allows us to start to answer these key questions. First we find that E_p has an average annual value of 1064.9 mm as compared to EC at 612.5 mm (Table 7). By including individual SWC profiles (TP 1 to 4) and the CRNP in the VZM framework we are able to constrain our estimate of E_a to between 525.3 and 643.1 mm and reduce E_a RMSE from 1.992 mm/day to around 1 mm/day (Table 6). In addition, a range of soil hydraulic parameters for each depth and spatially averaged top layer can be estimated to help better constrain recharge fluxes simultaneously. Given the principle of equifinality in hydrologic systems, the VZM framework may lead to equally reasonable estimates of parameters which is a limitation of the method and LSMs in general. Based on our sensitivity analysis (Figure 10) the key parameters of α , n may greatly affect E_a .

Although sparsely distributed, widespread state, national, and global meteorological observations paired with SWC profiles (Xia et al. 2015) and the VZM framework provide an opportunity to better constrain E_a and local soil hydraulic functions. Moreover, where multiple SWC profile information is available a range of E_a and soil hydraulic parameters can be estimated and thus considered in LSM data assimilation frameworks. The combination of basic meteorological observations with a CRNP in the VZM framework further allows for estimates of upscaled soil hydraulic parameters with similar estimates of E_a as found with individual SWC profiles. Moving forward, combining CRNP with deeper SWC observations from point sensors seems to be a reasonable strategy in order to average the inherent SWC variability in the near surface yet provide SWC constraints at depth, particularly as annual crops develop over the growing season.”

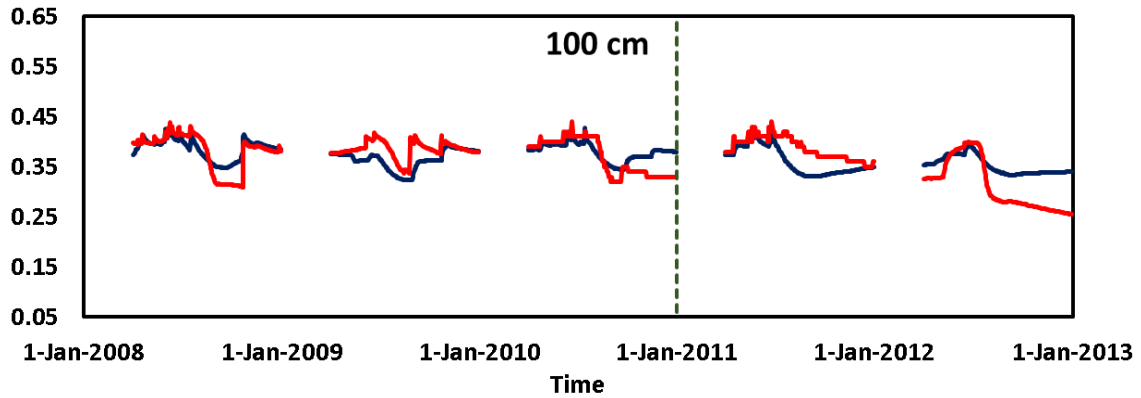
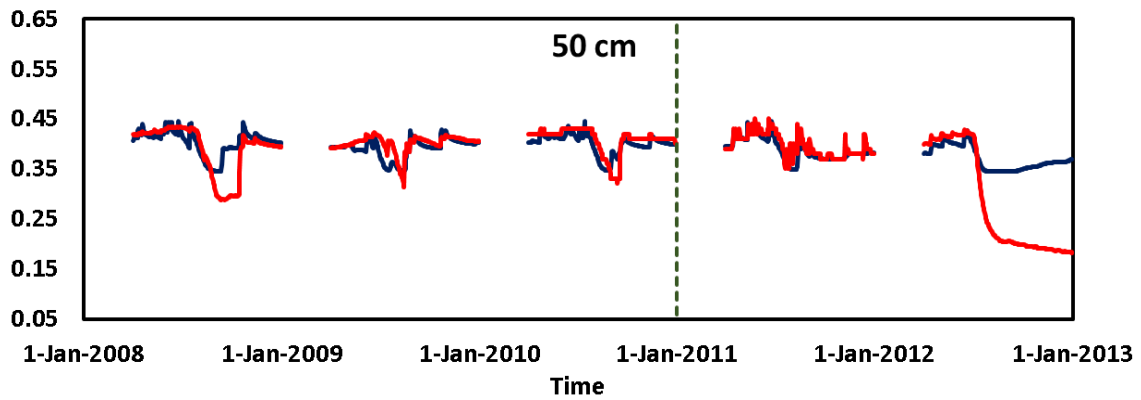
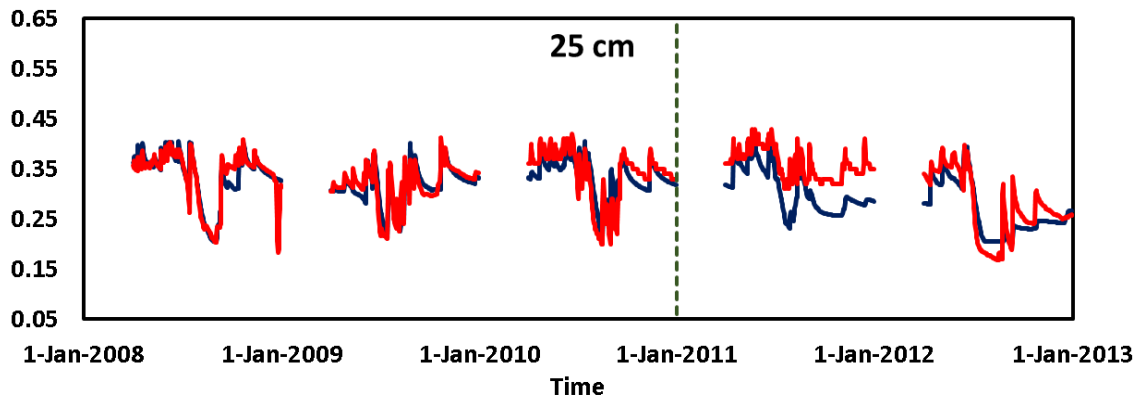
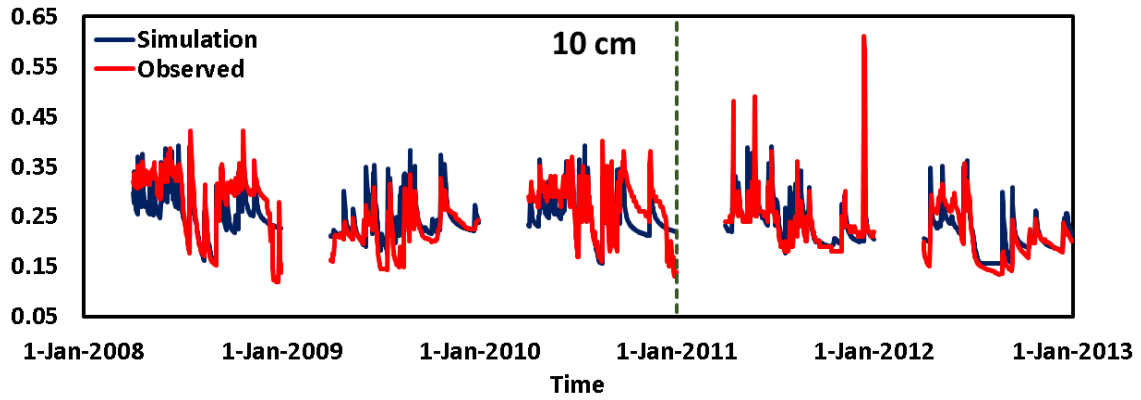
In Figure 4- Why standard deviations of water content in deeper soil layers are higher than shallow soil layers? As reviewer 1, suggested it would be worthwhile to try calibrating deeper soil layers first and then focus on shallow soil layers to assess model performance.

Thank you for your comment and sorry for the confusion. In Figure 4 we tried to show the temporal SWC variability throughout the field. It simply shows at a certain time we have higher SWC differences in deeper layers at different locations as compared to the upper layers.

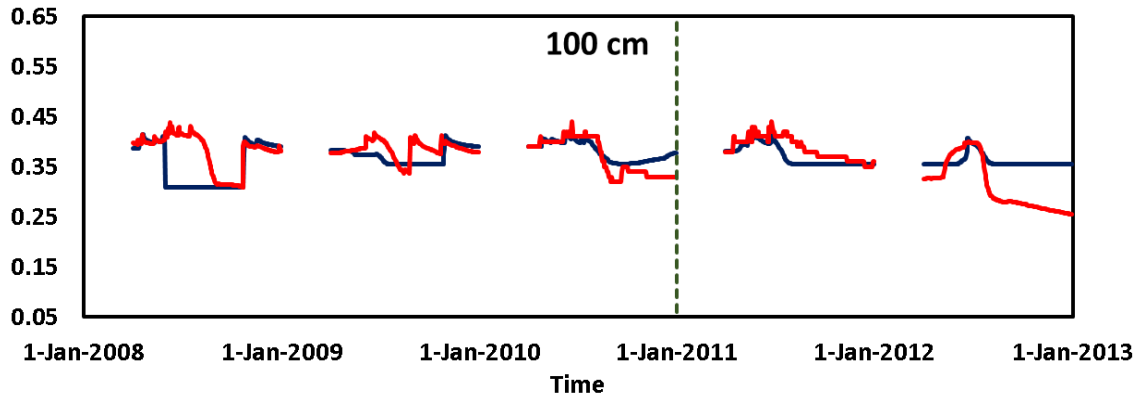
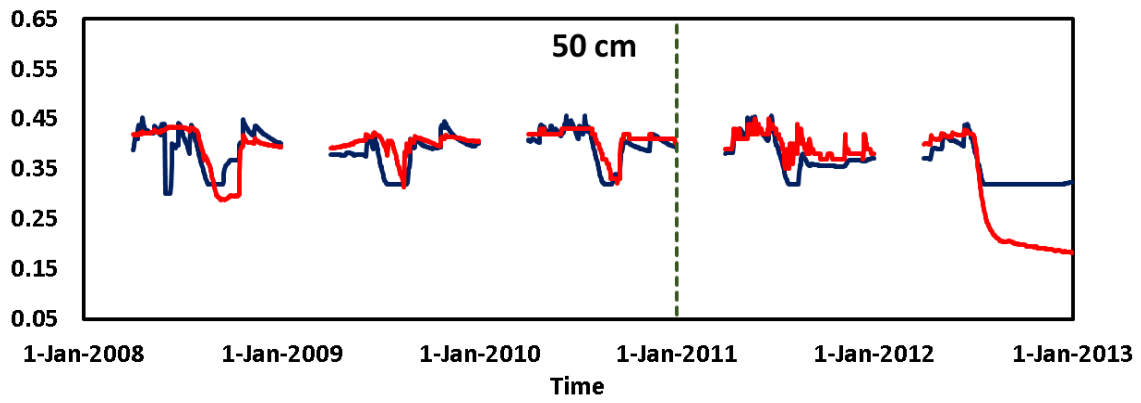
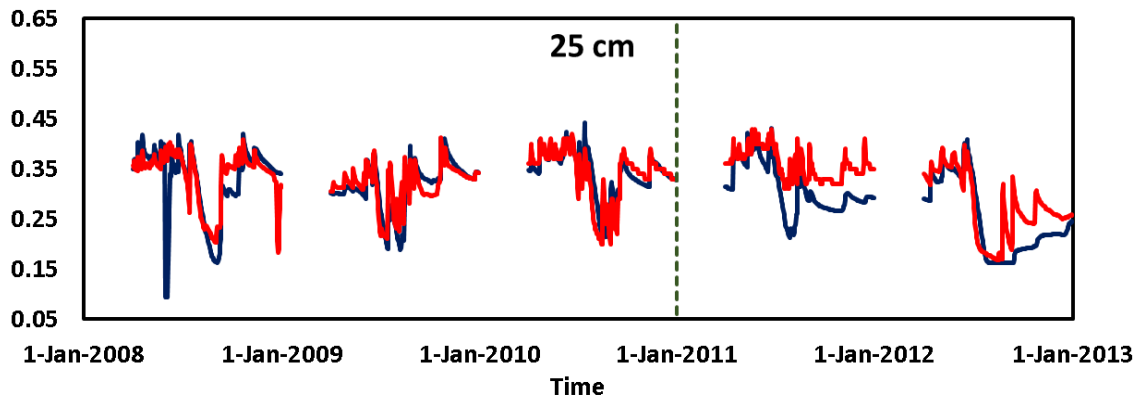
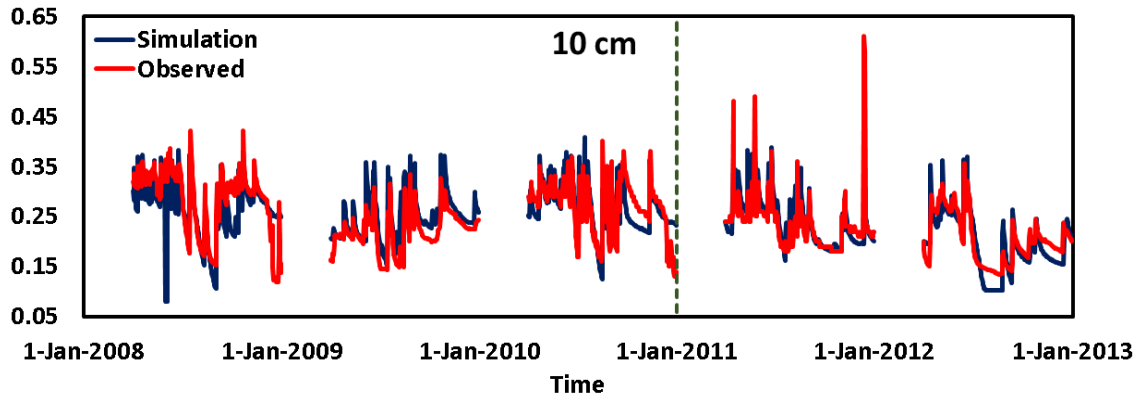
In order to see if your suggestion could improve the calibration and ET estimation results, we calibrated the model from the deeper layers to the upper layers at TP 1 location. As you can see in the tables and figures below, during both calibration and validation periods the ET estimation had poorer results as shown by the RMSE.

Optimization from top layers to the lower layers									
Location	Depth (cm)	Calibration Period (2008-2010)				Validation Period (2011-2012)			
		R ²	MAE	RMSE	NSE	R ²	MAE	RMSE	NSE
Mead 1	10	0.542	0.024	0.036	0.533	0.532	0.016	0.033	0.503
	25	0.742	0.014	0.022	0.739	0.716	0.029	0.040	0.486
	50	0.409	0.013	0.023	0.407	0.603	0.041	0.074	0.157
	100	0.352	0.015	0.022	0.343	0.419	0.027	0.038	0.358

Optimization from lower layers to the top layers									
Location	Depth (cm)	Calibration Period (2008-2010)				Validation Period (2011-2012)			
		R ²	MAE	RMSE	NSE	R ²	MAE	RMSE	NSE
Mead 1	10	0.466	0.024	0.039	0.438	0.591	0.018	0.034	0.471
	25	0.529	0.018	0.035	0.327	0.724	0.033	0.046	0.329
	50	0.405	0.017	0.028	0.121	0.677	0.037	0.060	0.456
	100	0.117	0.018	0.033	-0.451	0.362	0.027	0.042	0.193



Soil Hydraulic Parameters Optimization from top layers to the lower layers



Soil Hydraulic Parameters Optimization from lower layers to the top layers

ET Estimation from top layers to the lower layers			
Goodness-of-fit measures for simulated and observed Evapotranspiration (TP1)			
R²	MAE	RMSE	NSE
0.652	0.696	1.062	0.618

ET Estimation from lower layers to the top layers			
Goodness-of-fit measures for simulated and observed Evapotranspiration (TP1)			
R²	MAE	RMSE	NSE
0.515	0.795	1.218	0.475

1 **Feasibility analysis of using inverse modeling for estimating field-scale evapotranspiration in**
2 **maize and soybean fields from soil water content monitoring networks**

3

4 Foad Foolad¹, Trenton E. Franz², Tiejun Wang^{2,3}, Justin Gibson², Ayse Kilic^{1,2}, Richard G. Allen⁴,
5 Andrew Suyker²

6

7 ¹Civil Engineering Department, University of Nebraska-Lincoln, USA

8 ²School of Natural Resources, University of Nebraska-Lincoln, USA

9 ³Institute of Surface-Earth System Science, Tianjin University, P.R. China

10 ⁴Kimberly Research and Extension Center, University of Idaho, USA

11

12 **Keywords:** Evapotranspiration; Soil Water Content; Inverse Modeling; Soil Hydraulic Parameters;
13 Cosmic-Ray Neutron Probe

14 Corresponding author T.E. Franz (tfranz2@unl.edu)

15

16

17

18

19 **Abstract**

20 In this study the feasibility of using inverse vadose zone modeling for estimating field scale actual
21 evapotranspiration (ET_a) was explored at a long-term agricultural monitoring site in eastern
22 Nebraska. Data from both point scale soil water content (SWC) sensors and the area-average
23 technique of Cosmic-Ray Neutron Probes were evaluated against independent ET_a estimates from
24 a co-located Eddy-Covariance tower. While this methodology has been successfully used for
25 estimates of groundwater recharge, it was essential to assess the performance of other components
26 of the water balance such as ET_a . In light of recent evaluations of Land Surface Models (LSM)

Deleted: the

27 independent estimates of hydrologic state variables and fluxes are critically needed benchmarks.

Deleted: performance from the plumber experiment,

28 The results here indicate reasonable estimates of daily and annual ET_a from the point sensors, but
29 with highly varied soil hydraulic function parameterizations due to local soil texture variability.

30 The results of multiple soil hydraulic parameterizations leading to equally good ET_a estimates is
31 consistent with the hydrological principle of equifinality. While this study focused on one
32 particular site, the framework can be easily applied to other SWC monitoring networks across the
33 globe. The value added products of groundwater recharge and ET_a flux from the SWC monitoring
34 networks will provide additional and more robust benchmarks for the validation of LSM that
35 continues to improve their forecast skill. In addition, the value added products of groundwater
36 recharge and ET_a often have more direct impacts on societal decision making than SWC alone.
37 Water flux impacts human decision making from policies on the long-term management of
38 groundwater resources (recharge), to yield forecasts (ET_a), and to optimal irrigation scheduling
39 (ET_a). Illustrating the societal benefits of SWC monitoring is critical to insure the continued
40 operation and expansion of these public datasets.

41

44 1. Introduction

45 Evapotranspiration (ET) is an important component in terrestrial water and surface energy
46 balance. In the United States, ET comprises about 75% of annual precipitation, while in arid and
47 semiarid regions ET comprises more than 90% of annual precipitation (Zhang et al., 2001; Glenn
48 et al., 2007; Wang et al., 2009a). As such, an accurate estimation of ET is critical in order to
49 predict changes in hydrological cycles and improve water resource management (Suyker et al.,
50 2008; Anayah and Kaluarachchi, 2014). Given the importance of ET , an array of measurement
51 techniques at different temporal and spatial scales have been developed (c.f., Maidment, 1992;
52 Zhang et al., 2014), including lysimeter, Bowen ratio, Eddy-Covariance (EC), and satellite-based
53 surface energy balance approaches. However, simple, low-cost, and accurate field-scale
54 measurements of actual ET (ET_a) still remain a challenge due to the uncertainties of available
55 estimation techniques (Wolf et al., 2008; Li et al., 2009; Senay et al., 2011; Stoy, 2012). For
56 instance, field techniques, such as EC and Bowen ratio, can provide relatively accurate estimation
57 of local ET_a , but are often cost prohibitive for wide-spread use beyond research applications
58 (Baldocchi et al., 2001; Irmak, 2010). By comparison, satellite-based remote sensing techniques
59 are far less costly for widespread spatial coverage (Allen et al., 2007), but are limited by their
60 accuracy, temporal sampling frequency (e.g., Landsat 8 has a 16-day overpass), and technical
61 issues that further limit temporal sampling periods (e.g., cloud coverage during overpass) (Chemin
62 and Alexandridis, 2001; Xie et al., 2008; Li et al., 2009; Kjaersgaard et al., 2012).

63 As a complement to the above mentioned techniques, recent studies have used process-
64 based vadose zone models (VZMs) for estimating field-scale ET_a with reasonable success,
65 particularly in arid and semi-arid areas (Twarakavi et al., 2008; Izadifar and Elshorbagy, 2010;
66 Galleguillos et al., 2011; Wang et al., 2016). Although VZMs are time and cost effective for

67 estimating field-scale ET_a , they generally require complex model parameterizations and inputs,
68 some of which are not readily available (e.g., soil hydraulic parameters and plant physiological
69 parameters; c.f. Wang et al., 2016). In order to address the issue of missing soil hydraulic
70 parameters, a common approach is to use pedotransfer functions to convert readily available soil
71 information (e.g., texture, bulk density, etc.) to soil hydraulic parameters (Wösten et al., 2001);
72 however, significant uncertainties are usually associated with this method for estimating local
73 scale water fluxes (Wang et al., 2015). In fact, Nearing et al. (2016) identified soil hydraulic
74 property estimation as the largest source of information lost when evaluating different land surface
75 modeling schemes versus a soil moisture benchmark. Poor and uncertain parameterization of soil
76 hydraulic properties is a clear weakness of land surface models (LSMs) predictive skill in sensible
77 and latent heat fluxes (Best et al., 2015). This problem will continue to compound with the
78 continuing spatial refinement of hyper-resolution LSM grid cells to less than 1 km (Wood et al.,
79 2011).

80 In order to address the challenge of field scale estimation of soil hydraulic properties, here
81 we utilize inverse modeling for estimating soil hydraulic parameters based on field measurements
82 of soil water content (SWC) (c.f. Hopmans and Šimunek, 1999; Ritter et al., 2003). While VZM-
83 based inverse approaches have already been examined for estimating groundwater recharge (e.g.,
84 Jiménez-Martínez et al., 2009; Andreasen et al., 2013; Min et al., 2015; Ries et al., 2015;
85 Turkeltaub et al., 2015; Wang et al., 2016), its application for ET_a estimation has not been
86 adequately tested. Moreover, we note that simultaneous estimation of SWC states and surface
87 energy fluxes within LSMs is complicated by boundary conditions, model parameterization, and
88 model structure (Nearing et al., 2016). With the incorporation of regional soil datasets in LSMs
89 like Polaris (Chaney et al., 2016), effective strategies for estimating ground truth soil hydraulic

Deleted: modeling

91 properties from existing *SWC* monitoring networks (e.g., SCAN, CRN, COSMOS, State/National
92 Mesonets, c.f. Xia et al. (2015)) will become critical for continuing to improve the predictive skill
93 of LSMs.

94 The aim of this study is to examine the feasibility of using inverse VZM for estimating
95 field scale ET_a based on long-term local meteorological and *SWC* observations for an Ameriflux
96 (Baldocchi et al., 2001) EC site in eastern Nebraska, USA. We note that while this study focused
97 on one particular study site in eastern Nebraska, the methodology can be easily adapted to a
98 variety of *SWC* monitoring networks across the globe (Xia et al., 2015), thus providing an
99 extensive set of benchmark data for use in LSMs. The remainder of the paper is organized as
100 follows. In the methods section we will describe the widely used VZM, Hydrus-1D (Šimunek et al.,
101 2013), used to obtain soil hydraulic parameters. We will assess the feasibility of using both
102 profiles of in-situ *SWC* probes as well as the area-average *SWC* technique from Cosmic-Ray
103 Neutron Probes (CRNP). In the results section we will compare simulated ET_a resulted from
104 calibrated VZM with independent ET_a estimates provided by EC observations. Finally, a
105 sensitivity analysis of key soil and plant parameters will be presented.

Deleted: modeling

Deleted: Finally

106

107 2. Materials and Methodology

108 2.1 Study Site

109 The study site is located in eastern Nebraska, USA at the University of Nebraska
110 Agricultural and Development Center near Mead. The field site (US-Ne3, Figure 1a, 41.1797° N,
111 96.4397° W) is part of the Ameriflux Network (Baldocchi et al., 2001) and has been operating
112 continually since 2001. The regional climate is of a continental semiarid type with a mean annual

115 precipitation of 784 mm/year (according to the Ameriflux US-Ne3 website). According to the Web
116 Soil Survey Data (Soil Survey Staff, 2016, <http://websoilsurvey.nrcs.usda.gov/>), the soils at the site
117 are comprised mostly of silt loam and silty clay loam (Figure 1b and Table 1). Soybean and maize
118 are rotationally grown at the site under rainfed conditions, with the growing season beginning in
119 early May and ending in October (Kalfas et al., 2011). Since 2001, crop management practices (i.e.,
120 planting density, cultivars, irrigation, and herbicide and pesticide applications) have been applied
121 in accordance with standard best management practices prescribed for production-scale maize
122 systems (Suyker et al., 2008). More detailed information about site conditions can be found in
123 Suyker et al. (2004) and Verma et al. (2005).

124 An EC tower was constructed at the center of the field (Figure 1 and Figure 2a), which
125 continuously measures water, energy, and CO₂ fluxes (e.g., Baldocchi et al., 1988). At this field,
126 sensors are mounted at 3.0 m above the ground when the canopy is shorter than 1.0 m. At canopy
127 heights greater than 1.0 m, the sensors are then moved to a height of 6.2 m until harvest in order to
128 have sufficient upwind fetch (in all directions) representative of the cropping system being studied
129 (Suyker et al., 2004). In this study, hourly latent heat flux measurements were integrated to daily
130 values and then used for calculating daily EC ET_a integrated over the field scale. Detailed
131 information on the EC measurements and calculation procedures for ET_a are given in Suyker and
132 Verma (2009). Hourly air temperature, relative humidity, horizontal wind speed, net radiation, and
133 precipitation were also measured at the site. Destructive measurements of leaf area index (LAI)
134 were made every 10 to 14 days during the growing season at the study site (Suyker et al., 2005).
135 We note that the LAI data were linearly interpolated to provide daily estimates. Theta probes (TP)
136 (Delta-T Devices, Cambridge, UK) were installed at 4 locations in the study field with
137 measurement depths of 10, 25, 50, and 100 cm at each location to monitor hourly SWC in the root

138 zone (Suyker et al., 2008). Here, we denote these four locations as TP 1 (41.1775° N, 96.4442° W),
139 TP 2 (41.1775° N, 96.4428° W), TP 3 (41.1775° N, 96.4402° W), and TP 4 (41.1821° N, 96.4419°
140 W) (Figure 1b). Daily precipitation (P) and reference evapotranspiration (ET_r) computed for the
141 tall (alfalfa) reference crop using the ASCE standardized Penman-Monteith equation (ASCE-
142 EWRI 2005) are shown in Figure 3 for the study period (2007–2012) at the study site.

143 In addition, a CRNP (model CRS 2000/B, HydroInnova LLC, Albuquerque, NM, USA,
144 41.1798 N°, 96.4412° W) was installed near the EC tower (Figure 1b and 2b) on 20 April 2011.
145 The CRNP measures hourly moderated neutron counts (Zreda et al., 2008, 2012), which are
146 converted into SWC following standard correction procedures and calibration methods (c.f., Zreda
147 et al., 2012). In addition, the changes in above-ground biomass were removed from the CRNP
148 estimates of SWC following Franz et al. (2015). The CRNP measurement depth (Franz et al., 2012)
149 at the site varies between 15–40 cm, depending on SWC . Note for simplicity in this analysis we
150 assume the CRNP has an effective depth of 20 cm (mean depth of 10 cm) for all observational
151 periods. The areal footprint of the CRNP is $\sim 250 \pm 50$ m radius circle (see Desilets and Zreda
152 2013 and Köhli et al., 2015 for details). Here we assume for simplicity the EC and CRNP
153 footprints are both representative of the areal-average field conditions.

154

155 **2.2. Model setup**

156 **2.2.1 Vadose Zone Model**

157 The Hydrus-1D model (Šimunek et al., 2013), which is based on the Richards equation,
158 was used to calculate ET_a . The setup of the Hydrus-1D model is explained in detail by Jiménez-
159 Martínez et al. (2009), Min et al. (2015), and Wang et al. (2016), and only a brief description of

160 the model setup is provided here. Given the measurement depths of the Theta Probes, the
161 simulated soil profile length was chosen to be 175 cm with 176 nodes at 1 cm intervals. An
162 atmospheric boundary condition with surface runoff was selected as the upper boundary. This
163 allowed the occurrence of surface runoff when precipitation rates were higher than soil infiltration
164 capacity or if the soil became saturated. According to a nearby USGS monitoring well (Saunders
165 County, NE, USGS 411005096281502, ~2.7 km away), the depth to water tables was greater than
166 12 m during the study period. Therefore, free drainage was used as the lower boundary condition.

167 ~~Based on ASCE Penman-Monteith equation, ET_r values can be computed for either grass~~
168 ~~or alfalfa and then using crop-specific coefficients daily potential evapotranspiration (ET_p) can be~~
169 ~~calculated. Here ET_r values were calculated for the tall (0.5 m) ASCE reference (ASCE-~~
170 EWRI, 2005), and daily potential evapotranspiration (ET_p) was calculated according to FAO 56
171 (Allen et al., 1998):

$$172 \quad ET_p(t) = K_c(t) \times ET_r(t) \quad (1)$$

173 where K_c is a crop-specific coefficient at time t . The estimates of growth stage lengths and K_c
174 values for maize and soybean suggested by Allen et al. (1998) and Min et al. (2015) were adopted
175 in this study. In order to partition daily ET_p into potential transpiration (T_p) and potential
176 evaporation (E_p) as model inputs, Beer's law (Šimunek et al., 2013) was used as follows:

$$177 \quad E_p(t) = ET_p(t) \times e^{-k \times LAI(t)} \quad (2)$$

$$178 \quad T_p(t) = ET_p(t) - E_p(t) \quad (3)$$

Deleted: D
Formatted: Font:Not Italic
Deleted: was
Deleted: using the ASCE Penman-Monteith equation

182 where k [-] is an extinction coefficient with a value set to 0.5 (Wang et al., 2009b) and LAI [L^2/L^2]
 183 is leaf area index described in the previous section. The root water uptake, $S(h)$, was simulated
 184 according to the model of Feddes et al. (1978):

$$185 \quad S(h) = \alpha(h) \times S_p \quad (4)$$

186 where $\alpha(h)$ [-] is the root-water uptake water stress response function and varies between 0 and 1
 187 depending on soil matric potentials, and S_p is the potential water uptake rate and assumed to be
 188 equal to T_p . The summation of actual soil evaporation and actual transpiration is ET_a .

189 Since the study site has annual cultivation rotations between soybean and maize, the root
 190 growth model from the Hybrid-Maize Model (Yang et al., 2004) was used to model the root
 191 growth during the growing season:

$$192 \quad \begin{cases} \text{if } D < MRD, D = \frac{AGDD}{GDD_{silking}} MRD \\ \text{or } D = MRD \end{cases} \quad (5)$$

193 where D (cm) is plant root depth for each growing season day, MRD is the maximum root depth
 194 (assumed equal to 150 cm for maize and 120 cm for soybean in this study following Yang et al.,
 195 2004), $AGDD$ is the accumulated growing degree days, and $GDD_{silking}$ is the accumulated GDD at
 196 the silking point (e.g., accumulated plant GDD approximately 60-70 days after crop emergence).
 197 GDD for each growing season day was calculated as:

$$198 \quad GDD = \frac{T_{max} - T_{min}}{2} - T_{base} \quad (6)$$

199 where T_{max} and T_{min} are the maximum and minimum daily temperature ($^{\circ}C$), respectively, and T_{base}
 200 is the base temperature set to be $10^{\circ} C$ following McMaster and Wilhelm (1997) and Yang et al.

Deleted:

202 (1997). Finally, the Hoffman and van Genuchten (1983) model was used to calculate root
203 distribution. Further details about the model can be found in Šimunek et al. (2013).

204

205 2.2.2 Inverse modeling to estimate soil hydraulic parameters

206 Inverse modeling was used to estimate soil hydraulic parameters for the van Genuchten-
207 Mualem model (Mualem, 1976; van Genuchten, 1980):

$$208 \theta(h) = \begin{cases} \theta_r + \frac{\theta_s - \theta_r}{(1 + |\alpha h|)^m}, & h < 0 \\ \theta_s, & h \geq 0 \end{cases} \quad (7)$$

$$209 K(S_e) = K_s \times S_e^l \times [1 - (1 - S_e^{1/m})^m]^2 \quad (8)$$

210 where θ [L^3/L^3] is volumetric *SWC*; θ_r [L^3/L^3] and θ_s [L^3/L^3] are residual and saturated water
211 content, respectively; h [L] is pressure head; K [L/T] and K_s [L/T] are unsaturated and saturated
212 hydraulic conductivity, respectively; and $S_e (= (\theta - \theta_r) / (\theta_s - \theta_r))$ [-] is saturation degree. With respect
213 to the fitting factors, α [1/L] is inversely related to air entry pressure, n [-] measures the pore size
214 distribution of a soil with $m=1-1/n$, and l [-] is a parameter accounting for pore space tortuosity
215 and connectivity.

Deleted: moisture

216 Daily *SWC* data from the four TP locations and CRNP location were used for the inverse
217 modeling. Based on the measurement depths of the TPs, the simulated soil columns were divided
218 into four layers for TP locations (i.e., 0-15 cm, 15-35 cm, 35-75 cm, and 75-175 cm), which led to
219 a total of 24 hydraulic parameters (θ_r , θ_s , α , n , K_s , and l) to be optimized based on observed *SWC*
220 values. In order to efficiently optimize the parameters, we used the method outlined in Turkeltaub
221 et al. (2015). Since Hydrus-1D is limited to optimizing a maximum of 15 parameters at once and

223 that the *SWC* of the lower layers changes more slowly and over a smaller range than the upper
224 layers, the van Genuchten parameters of the upper two layers were first optimized, while the
225 parameters of the lower two layers were fixed. Then, the optimized van Genuchten parameters of
226 the upper two layers were kept constant, while the parameters of the lower two layers were
227 optimized. The process was continued until there were no further improvements in the optimized
228 hydraulic parameters or until the changes in the lowest sum of squares were less than 0.1%. Given
229 the sensitivity of the optimization results to the initial guesses of soil hydraulic parameters in the
230 Hydrus model, soil hydraulic parameters from six soil textures were used as initial inputs for the
231 optimizations at each location (Carsel and Parish, 1988), including sandy clay loam, silty clay
232 loam, loam, silt loam, silt, and clay loam. Based on the length of available *SWC* data from the TP
233 measurements, the periods of 2007, 2008-2010, and 2011-2012 were used as the spin-up,
234 calibration, and validation periods, respectively. Moreover, to minimize the impacts of freezing
235 conditions on the quality of *SWC* measurements, data from January to March of each calendar year
236 were removed (based on available soil temperature data) from the optimizations.

237 In addition to the TP profile observations, we used the CRNP area-average *SWC* in the
238 inverse procedure to develop an independent set of soil parameters. The CRNP was assumed to
239 provide *SWC* data with an average effective measurement depth of 20 cm at this study site. The
240 observation point was therefore set at 10 cm. As a first guess and in the absence of other
241 information, soil properties were assumed to be homogeneous throughout the simulated soil
242 column with a length of 175 cm. Because the CRNP was installed in 2011 at the study site, the
243 periods of 2011, 2012-2013, and 2014 were used as spin-up, calibration, and validation periods,
244 respectively, for the optimization procedure.

245 The lower and upper bounds of each van Genuchten parameter are provided in Table 2.
 246 With respect to the goodness-of-fit assessment, Root Mean Square Error (RMSE) between
 247 simulated and observed *SWC* was chosen as the objective function to minimize in order to estimate
 248 the soil hydraulic parameters. The built in optimization procedure in Hydrus-1D was used to
 249 perform parameter estimation. A sensitivity analysis of the six soil model parameters was
 250 performed. In addition, three additional performance criteria, including Coefficient of
 251 Determination (R^2), Mean Average Error (MAE), and the Nash-Sutcliffe Efficiency (NSE) were
 252 used to further evaluate and validate the selected model behavior:

$$253 \quad RMSE = \sqrt{\frac{1}{n} \sum_{i=1}^n (P_i - O_i)^2} \quad (9)$$

$$254 \quad R^2 = \left(\frac{n(\sum_{i=1}^n P_i O_i) - (\sum_{i=1}^n P_i)(\sum_{i=1}^n O_i)}{\sqrt{[n \sum_{i=1}^n P_i^2 - (\sum_{i=1}^n P_i)^2][n \sum_{i=1}^n O_i^2 - (\sum_{i=1}^n O_i)^2]}} \right)^2 \quad (10)$$

$$255 \quad MAE = \frac{1}{n} \sum_{i=1}^n |P_i - O_i| \quad (11)$$

$$256 \quad NSE = 1 - \frac{\sum_{i=1}^n (P_i - O_i)^2}{\sum_{i=1}^n (O_i - \bar{O}_i)^2} \quad (12)$$

257 where n is the total number of *SWC* data points, O_i , and P_i , are respectively the observed and
 258 simulated daily *SWC* on day i , and \bar{O}_i is the observed mean value. Based on the best scores (i.e.,
 259 lowest RMSE values), the best optimized set of soil hydraulic parameters at each location were
 260 selected. Using the selected parameters, the Hydrus model was then run in a forward mode in order
 261 to estimate ET_a between 2007 and 2012. Finally, we note that the years 2004-2006 were used as a
 262 model spin-up period for the forward model and evaluation of ET_a because of the longer climate
 263 record length.

264

265 **3. Results and Discussions**

266 **3.1 Vadose Zone Inverse Modeling Results**

267 The time series of the average *SWC* from the four TP locations along with one standard
268 deviation at each depth are plotted in Figure 4. Based on the large spatial standard deviation values
269 (Figure 4), despite the relatively small spatial scale (~65 ha) and uniform cropping at the study site,
270 *SWC* varies considerably across the site, particularly during the growing season. The comparison
271 between *SWC* data from the CRNP and spatial average of *SWC* data at the four TP locations in the
272 study field (i.e. average of 10 and 25 cm depths at TP locations) is presented in Figure 5. The daily
273 RMSE between the spatial average of the TPs and CRNP data is $0.037 \text{ cm}^3/\text{cm}^3$, which is
274 consistent with other studies that reported similar values in semiarid shrublands (Franz et al., 2012),
275 German Forests (Bogena et al., 2013, Baatz et al., 2014), montane forests in Utah (Lv et al., 2014),
276 sites across Australia (Hawdon et al., 2014), and a mixed land use agricultural site in Austria
277 (Franz et al. 2016). We note that we would expect lower RMSE ($\sim < 0.02 \text{ cm}^3/\text{cm}^3$) with additional
278 point sensors located at shallower depths and in more locations distributed across the study site.
279 Nevertheless, the consistent behavior between the spatial mean *SWC* of TPs and the CRNP allows
280 us to explore spatial variability of soil hydraulic properties within footprint using inverse modeling.
281 This will be described in the next sections. The study period (2007-2012, Figure 6) contained
282 significant inter-annual variability in precipitation. During the spin-up period in 2007, the annual
283 precipitation (942 mm) was higher than the mean annual precipitation (784 mm), 2008 was a wet
284 year (997 mm), 2009-2011 were near average years (715 mm), and 2012 was a record dry year
285 (427 mm) with widespread drought across the region. Therefore, both wet and dry years were
286 considered in the inverse modeling simulation period.

287 As an illustration, Figure 7 shows the daily observed and simulated *SWC* during the
288 calibration (2008–2010) and validation (2011–2012) periods at the TP 1 location (the simulation
289 results of the other three sites can be found in the supplemental Figures S1, S2, and S3). The
290 results of objective function criterion (RMSE) and the other three performance criteria (e.g., R^2 ,
291 ~~MAE, and~~ NSE) between simulated and observed *SWC* values at TPs locations are presented in
292 Table 3.

Deleted: MAE, and

293 In this research we define RMSE values less than $0.03 \text{ cm}^3/\text{cm}^3$ between observed and
294 simulated *SWC* values as well-matched and RMSE between 0.03 and $0.06 \text{ cm}^3/\text{cm}^3$ as fairly well-
295 matched. We note the target error range of satellite *SWC* products (e.g. SMOS and SMAP) is less
296 than $0.04 \text{ cm}^3/\text{cm}^3$ (Entekhabi et al., 2010). Similar to previous studies (e.g., Jiménez-Martínez et
297 al., 2009; Andreasen et al., 2013; Min et al., 2015; Wang et al., 2016), the results of all the
298 performance criteria at TP locations show the capability of inverse modeling in estimation of soil
299 hydraulic parameters. The results of the calibration period (2008-2010) indicate that the simulated
300 and observed *SWC* values are in good agreement (i.e. well matched as defined above) throughout
301 the entire period at most locations and depths (Figure 7 and Table 3). In addition, the simulated
302 and observed *SWC* data are fairly well-matched at most locations and depths during the validation
303 period (2011-2012), with notable differences during the second half of 2012 during the extreme
304 drought conditions (Figure 7 and Table 3). Reasons for this disagreement in the observed and
305 simulated *SWC* data will be discussed in the following sections.

306 The results of inverse modeling using the CRNP data also indicate the feasibility of using
307 these data to estimate effective soil hydraulic parameters (Figure 8 and Table 4). Based on the
308 performance criteria (Table 4), the simulated data are fairly well-matched with the observed *SWC*
309 data during both the calibration and validation periods. Additional information from deeper soil

311 probes or more complex modeling approaches such as data assimilation techniques (Rosolem et al.,
312 2014, Renzullo et al., 2014) may be needed to fully utilize the CRNP data for the entire growing
313 season. However, this was beyond the scope of the current study and merits further investigation
314 given the global network of CRNP (Zreda et al., 2012) dating back to ~2011.

315 Table 5 summarizes the optimized van Genuchten parameters for the four different depths
316 of the four TP locations and the single layer for the CRNP location. The optimized parameters
317 were then used to estimate ET_a for the entire study period as an independent comparison to the EC
318 ET_a data. The results of the ET_a evaluation will be discussed in the next section. According to the
319 simulation results (Table 5), in most of the soil layers, the TP 4 location results in lower n , K_s , and
320 higher θ_r values than the other 3 locations (TPs 1-3), suggesting either underlying soil texture
321 variability in the field or texture dependent sensor sensitivity/calibration. As a validation for the
322 simulation results, the publicly available Web Soil Survey Data
323 (<http://websoilsurvey.nrcs.usda.gov/>) was used to explore whether the optimized van Genuchten
324 parameters from the inverse modeling (Figure 1b and Table 2) agreed qualitatively with the survey
325 data. Based on the Web Soil Survey Data, the soil at the TP 4 location contains higher clay
326 percentage than the other locations. Meanwhile, the optimized parameters reflect the spatial pattern
327 of soil texture in the field as shown by the Web Soil Survey Data (e.g., lower n and K_s values and
328 higher θ_r values at the TP 4 location with finer soil texture). Physically, finer-textured soils
329 generally have lower K_s and higher θ_r values (Carsel and Parrish, 1988). Moreover, the shape
330 factor n is indicative of pore size distributions of soils. In general, finer soils with smaller pore
331 sizes tend to have lower n values (Carsel and Parrish, 1988). The observed SWC at the TP 4
332 location is consistently higher than the average SWC of the other three locations (Figure S4 in
333 supplemental materials), which can be partly attributed to the higher θ_r values at the TP 4 location

334 (Wang and Franz, 2015). Overall, the obtained van Genuchten parameters from the inverse
335 modeling are in qualitatively good agreement with the available spatial distribution of soil texture
336 in the study field, indicating the capability of using inverse VZM to infer soil hydraulic properties.
337 Further work on validating the Web Soil Survey Data soil hydraulic property estimates is of
338 general interest to the LSM community.

339

340 **3.2 Comparison of modeled ET_a with observed ET_a**

341 Because a longer set of climatic data was available at the study site (as compared to *SWC*
342 data), we used 2004-2006 as a spin-up period. Using the best fit soil hydraulic parameters for the
343 four TP locations and the single CRNP location, the Hydrus-1D model was then run in a forward
344 mode to calculate ET_a over the entire study period (2007-2012). The simulated daily ET_a was then
345 compared with the independent EC ET_a measurements using RMSE (Eq. (9)) as the evaluation
346 criterion. In order to upscale TP ET_a estimation to the field/EC scale, we used the soil textural
347 boundaries and areas defined by the Web Soil Survey Data map to compute a weighted average
348 ET_a . In this research we consider RMSE values less than 1 mm/day between observed and
349 simulated ET_a values as well-matched and RMSE values between 1 and 1.2 as fairly well-matched
350 (Figure 9 and Table 6). The performance criterion results indicate that the simulated daily ET_a is in
351 a better agreement with EC ET_a measurements at the TP 1-3 locations than at the TP 4 and CRNP
352 locations (Table 6). However, based on the performance criteria from inverse modeling results and
353 on the Web Soil Survey Data, we conclude that spatial heterogeneity of soil texture in the study
354 field results in significant spatial variation in ET_a rates across the field (e.g., less ET_a occurs at the
355 TP 4 location than from the other parts of the field). Here smaller ET_a rates at the TP 4 location are

356 likely due to finer soil texture at this location, which makes it more difficult for the plant/roots to
357 overcome potentials to extract water from the soil, thus leading to a lower ET_a rate and greater
358 plant stress. In addition, higher surface runoff can be expected at the TP 4 location due to finer-
359 textured soils (as we observed during our field campaigns). According to the simulation results the
360 average surface runoff at the TP 4 location was about 44.8 mm/year from 2007 to 2012, while the
361 average surface runoff at the other three locations (TPs 1-3) was around 10.6 mm/year, which
362 partially accounts for the lower ET_a rates. We note that future work using historic yield maps may
363 also be used to further elucidate the soil hydraulic property differences given the direct correlation
364 between transpiration and yield.

365 Given that CRNPs have a limited observational depth and that only one single soil layer
366 was optimized in the inverse model for the CRNP, one could expect the simulated daily ET_a from
367 the CRNP to have larger uncertainty. Here we found an RMSE of 1.14 mm/day using the CRNP
368 versus 0.91 mm/day for the upscaled TP locations. However, when the optimized soil parameters
369 obtained from the CRNP data were used to estimate ET_a , the model did simulate daily ET_a fairly
370 well during both non-growing and growing seasons in comparison to the EC ET_a measurements.

371 On the annual scale, ET_a measured by the EC tower accounted for 87% of annual P
372 recorded at the site during the study period (Figure 6). Overall, the simulated annual ET_a at all the
373 TP and CRNP locations is comparable to the annual ET_a measured by the EC tower, except during
374 2012 (Table 7), in which a severe drought occurred in the region. One explanation is that the plants
375 extract more water from deeper layers under extreme drought conditions than what we defined as a
376 maximum rooting depth (150 cm for maize and 120 cm for soybean) for the model, thus limiting
377 the VZM ability to estimate ET_a accurately during the drought year (2012). In fact, based on the
378 EC ET_a measurements at the study site, there was just 8.18% reduction in annual ET_a in 2012 than

379 the average of the other years (2007-2011), while there were 29.58% and 35.75% reduction in
380 annual simulated ET_a values respectively in upscaled TP and CRNP. This shows that although
381 2012 was a very dry year, the plants probably found most of the needed water by extracting water
382 from deeper soil reservoirs. As previously mentioned we defined a maximum rooting depth for the
383 model that could greatly impact the results. To further illustrate this point, a sensitivity analysis
384 was performed on the maximum rooting depth and presented in the following section. However,
385 we note that given the fact that EC ET_a estimation can have up to 20% uncertainty (Massman and
386 Lee, 2002, and Hollineger and Richardson, 2005), and accounting for the natural spatial variability
387 of ET_a due to soil texture and root depth growth uncertainties, the various ET_a estimation
388 techniques performed fairly well. In fact, it is difficult to identify which ET_a estimation method is
389 the most accurate method. These results are consistent with the concept of equifinality in
390 hydrologic modeling given the complexity of natural systems (Beven and Freer, 2001). Moreover,
391 the findings here are consistent with Nearing et al. (2016) that show information lost in model
392 parameters greatly affects the soil moisture comparisons against a benchmark. However, soil
393 parameterization was less important in the loss of information for the comparisons of ET /latent
394 energy against a benchmark. Fully resolving these issues remains a key challenge to the land
395 surface modeling community and the model's ability to make accurate predictions (Best 2015).
396 The following section provides a detailed sensitivity analysis of the soil hydraulic parameters and
397 root depth growth functions in order to begin to understand the sources of error in estimating ET_a
398 from SWC monitoring networks.

399

400 3.3 Sensitivity analysis of soil hydraulic parameters and rooting depth

401 In this research we compared simulated ET_a with the measured EC ET_a . As expected some
402 discrepancies between simulated and measured ET_a values existed. In order to begin to understand
403 the key sources of error we performed a set of sensitivity analysis experiments on the estimated
404 soil hydraulic parameters. Building on Wang et al. (2009b), a sensitivity analysis for a single
405 homogeneous soil layer (6 parameters) and a 4-layer soil profile (24 parameters) was performed
406 over the study period (2007–2012). Here we performed a preliminary sensitivity analysis by
407 changing a single soil hydraulic parameter one at a time while keeping the other parameters
408 constant (i.e. at the average value). Figure 10 illustrates the sensitivity results on simulated ET_a ,
409 indicating the soil hydraulic parameters have a range of sensitivities with tortuosity (l) being the
410 least. We found that n and α were the most sensitive, particularly in the shallowest soil layer. This
411 sensitivity to the shallowest soil layer provides an opportunity to use the CRNP observations,
412 particularly in the early growing season (i.e. when evaporation dominates latent energy flux), to
413 help constrain estimates of n and α . As the crop continues to develop (and transpiration contributes
414 a relatively larger component of latent energy) additional information about deeper soil layers
415 should be used to estimate soil hydraulic parameters or perform data assimilation. Moreover, the
416 CRNP may be useful in helping constrain and parameterize soil hydraulic functions in simpler
417 evaporation models widely used in remote sensing (c.f. Allen et al. 2007) and crop modeling (c.f.
418 Allen et al. 1998).

419 Following the sensitivity analysis, we repeated the optimization experiment using only α , n ,
420 K_s , and used model default estimates for the other parameters in each layer. We found that the
421 RMSE values were significantly higher (1.511 vs. 0.911 mm/day) than when considering all 24
422 parameters. We suspect that given the high correlation between soil hydraulic parameters (Carsel
423 and Parrish 1988), that fixing certain parameters leads to a degradation in overall performance. We

Deleted:

425 suggest further sensitivity analyses, in particular changing multiple parameters simultaneously or
426 using multiple objective functions, be used to fully understand model behavior (c.f. Bastidas et al.
427 1999 and Rosolem et al. 2012).

428 A sensitivity analysis of ET_a by varying rooting depth is summarized in Figure 11. As
429 would be expected with increasing rooting depth, higher ET_a occurred. In addition, Figure 11
430 illustrates a decreasing RMSE against EC observations for up to 200% increases. Again it is
431 unclear if the EC observations are biased high or in fact rooting depths are much greater than
432 typically considered in these models. The high observed EC values in the drought year of 2012
433 indicate that roots likely uptake water from below the 1 m observations. Certainly the results
434 shown here further indicate the importance of root water uptake parameters in VZMs and LSMs,
435 even in homogeneous annual cropping systems. While beyond the scope of this paper we refer the
436 reader to the growing literature on the importance of root water uptake parameters on hydrologic
437 fluxes (c.f. Schymanski et al. 2008 and Guswa 2012).

438

439 **3.4 Applications and limitations of the vadose zone modeling framework**

440 Given its simplicity and widespread availability of ground data, ET_c and K_c values are
441 often used in a wide variety of applications to estimate ET_p and thus approximate ET_a . It is well
442 known that SWC is a limiting factor affecting the assumption that $ET_p \sim ET_c$. On the other hand,
443 we know that SWC observations are local in nature and not necessarily representative of ET_p
444 footprint estimates. The key questions are: what is the value of SWC observations, how many
445 profiles do we need to install in a footprint, and at which depths to constrain estimates of fluxes?
446 The well instrumented and long-term study presented here allows us to start to answer these key

Formatted: Font:Italic
Formatted: Font:Italic, Subscript
Formatted: Font:Italic
Formatted: Font:Italic
Formatted: Font:Italic, Subscript
Formatted: Font:Italic
Formatted: Font:Italic, Subscript
Formatted: Font:Italic
Formatted: Font:Italic
Formatted: Font:Italic, Subscript
Formatted: Font:Italic
Formatted: Font:Italic
Formatted: Font:Italic, Subscript
Formatted: Font:Italic

447 questions. First we find that ET_a has an average annual value of 1064.9 mm as compared to EC at
448 612.5 mm (Table 7). By including individual SWC profiles (TP 1 to 4) and the CRNP in the VZM
449 framework we are able to constrain our estimate of ET_a to between 525.3 and 643.1 mm and
450 reduce ET_a RMSE from 1.992 mm/day to around 1 mm/day (Table 6). In addition, a range of soil
451 hydraulic parameters for each depth and spatially averaged top layer can be estimated to help
452 better constrain recharge fluxes simultaneously. Given the principle of equifinality in hydrologic
453 systems, the VZM framework may lead to equally reasonable estimates of parameters which is a
454 limitation of the method and LSMs in general. Based on our sensitivity analysis (Figure 10) the
455 key parameters of α , n may greatly affect ET_a .

Formatted: Font:Italic

Formatted: Font:Italic, Subscript

Formatted: Font:Italic

Formatted: Font:Italic, Subscript

456 Although sparsely distributed, widespread state, national, and global meteorological
457 observations paired with SWC profiles (Xia et al. 2015) and the VZM framework provide an
458 opportunity to better constrain ET_a and local soil hydraulic functions. Moreover, where multiple
459 SWC profile information is available a range of ET_a and soil hydraulic parameters can be
460 estimated and thus considered in LSM data assimilation frameworks. The combination of basic
461 metrological observations with a CRNP in the VZM framework further allows for estimates of
462 upscaled soil hydraulic parameters with similar estimates of ET_a as found with individual SWC
463 profiles. Moving forward, combining CRNP with deeper SWC observations from point sensors
464 seems to be a reasonable strategy in order to average the inherent SWC variability in the near
465 surface yet provide SWC constraints at depth, particularly as annual crops develop over the
466 growing season.

Formatted: Font:Italic

Formatted: Font:Italic, Subscript

Formatted: Font:Italic

Formatted: Font:Italic, Subscript

467

468 4. Conclusions

469 In this study the feasibility of using inverse vadose zone modeling for field scale ET_a
470 estimation was explored at an agricultural site in eastern Nebraska. Both point SWC sensors (TP)
471 and area-average techniques (CRNP) were explored. This methodology has been successfully used
472 for estimates of groundwater recharge but it was critical to assess the performance of other
473 components of the water balance such as ET_a . The results indicate reasonable estimates of daily
474 and annual ET_a but with varied soil hydraulic function parameterizations. The varied soil hydraulic
475 parameters were expected given the heterogeneity of soil texture at the site and consistent with the
476 principle of equifinality in hydrologic systems. We note that while this study focused on one
477 particular site, the framework can be easily applied to other networks of SWC monitoring across
478 the globe (Xia et al., 2015). The value added products of groundwater recharge and ET_a flux from
479 the SWC monitoring networks will provide additional and more robust benchmarks for the
480 validation of LSM that continue to improve their forecast skill.

481

482 **5. Data availability**

483 The climatic and EC data used in this research can be found at <http://ameriflux.lbl.gov/>.
484 The TP SWC and LAI data in the study site are provided by Dr. Andrew Suyker and CRNP SWC
485 are provided by Dr. Trenton E. Franz and both sets of data can be requested directly from the
486 authors. The US soil taxonomy information is provided by Soil Survey Staff and is available
487 online at <http://websoilsurvey.nrcs.usda.gov/> (accessed in July, 2016). The remaining datasets are
488 provided in the supplemental material associated with this paper.

489

490 **Acknowledgments**

491 This research is supported financially by the Daugherty Water for Food Global Institute at
492 the University of Nebraska, NSF EPSCoR FIRST Award, the Cold Regions Research Engineering
493 Laboratory through the Great Plains CESU, and an USGS104b grant. We sincerely appreciate the
494 support and the use of facilities and equipment provided by the Center for Advanced Land
495 Management Information Technologies, School of Natural Resources and data from Carbon
496 Sequestration Program, the University of Nebraska-Lincoln. TEF would like to thank Eric Wood
497 for his inspiring research and teaching career. No doubt the skills TEF learned while at Princeton
498 in formal course work, seminars, and discussions with Eric will serve him well in his own career.

499 **References**

- 500 Allen, R. G., Pereira, L. S., Raes, D., & Smith, M. (1998). Crop evapotranspiration-guidelines for
501 computing crop water requirements-FAO irrigation and drainage paper 56. FAO, Rome,
502 300(9), D05109.
- 503 Allen, R. G., Tasumi, M., & Trezza, R. (2007). Satellite-based energy balance for mapping
504 evapotranspiration with internalized calibration (METRIC)—Model. *Journal of Irrigation and*
505 *Drainage Engineering*, 133(4), 380-394.
- 506 Anayah, F. M., & Kaluarachchi, J. J. (2014). Improving the complementary methods to estimate
507 evapotranspiration under diverse climatic and physical conditions. *Hydrology and Earth*
508 *System Sciences*, 18(6), 2049-2064.
- 509 Andreasen, M., Andreasen, L. A., Jensen, K. H., Sonnenborg, T. O., & Bircher, S. (2013).
510 Estimation of regional groundwater recharge using data from a distributed soil moisture
511 network. *Vadose Zone Journal*, 12(3)
- 512 ASCE – EWRI. (2005). The ASCE Standardized reference evapotranspiration equation. ASCE-
513 EWRI Standardization of Reference Evapotranspiration Task Comm. Report, ASCE
514 Bookstore, ISBN 078440805, Stock Number 40805, 216 pages.
- 515 Baatz, R., Bogena, H., Franssen, H. H., Huisman, J., Qu, W., Montzka, C., et al. (2014).
516 Calibration of a catchment scale cosmic-ray probe network: A comparison of three
517 parameterization methods. *Journal of Hydrology*, 516, 231-244.
- 518 Baldocchi, D. D., Hincks, B. B., & Meyers, T. P. (1988). Measuring biosphere-atmosphere
519 exchanges of biologically related gases with micrometeorological methods. *Ecology*, 1331-
520 1340.
- 521 Baldocchi, D., Falge, E., Gu, L., & Olson, R. (2001). FLUXNET: A new tool to study the temporal
522 and spatial variability of ecosystem-scale carbon dioxide, water vapor, and energy flux
523 densities. *Bulletin of the American Meteorological Society*, 82(11), 2415.

- 524 Bastidas, L. A., H. V. Gupta, S. Sorooshian, W. J. Shuttleworth, and Z. L. Yang (1999), Sensitivity
525 analysis of a land surface scheme using multicriteria methods, *J. Geophys. Res.-Atmos.*,
526 104(D16), 19481-19490. doi:10.1029/1999jd900155.
- 527 Best, M., Abramowitz, G., Johnson, H., Pitman, A., Balsamo, G., Boone, A., et al. (2015). The
528 plumbing of land surface models: Benchmarking model performance. *Journal of*
529 *Hydrometeorology*, 16(3), 1425-1442.
- 530 Beven, K., & Freer, J. (2001). Equifinality, data assimilation, and uncertainty estimation in
531 mechanistic modelling of complex environmental systems using the GLUE methodology.
532 *Journal of Hydrology*, 249(1), 11-29.
- 533 Bogena, H., Huisman, J., Baatz, R., Hendricks Franssen, H., & Vereecken, H. (2013). Accuracy of
534 the cosmic-ray soil water content probe in humid forest ecosystems: The worst case scenario.
535 *Water Resources Research*, 49(9), 5778-5791.
- 536 Carsel, R. F., & Parrish, R. S. (1988). Developing joint probability distributions of soil water
537 retention characteristics. *Water Resources Research*, 24(5), 755-769.
- 538 Chaney, N. W., Wood, E. F., McBratney, A. B., Hempel, J. W., Nauman, T. W., Brungard, C. W.,
539 et al. (2016). POLARIS: A 30-meter probabilistic soil series map of the contiguous United
540 States. *Geoderma*, 274, 54-67.
- 541 Chemin, Y., & Alexandridis, T. (2001). Improving spatial resolution of ET seasonal for irrigated
542 rice in Zhanghe, china. Paper Presented at the 22nd Asian Conference on Remote Sensing, 5.
543 pp. 9.
- 544 Desilets, D., & Zreda, M. (2013). Footprint diameter for a cosmic-ray soil moisture probe: Theory
545 and monte carlo simulations. *Water Resources Research*, 49(6), 3566-3575.
- 546 Entekhabi, D., E. G. Njoku, P. E. O'Neill, K. H. Kellogg, W. T. Crow, W. N. Edelstein, J. K.
547 Entin, S. D. Goodman, T. J. Jackson, J. Johnson, J. Kimball, J. R. Piepmeier, R. D. Koster, N.
548 Martin, K. C. McDonald, M. Moghaddam, S. Moran, R. Reichle, J. C. Shi, M. W. Spencer, S.

549 W. Thurman, L. Tsang, and J. Van Zyl (2010), The Soil Moisture Active Passive (SMAP)
550 Mission, Proc. IEEE, 98(5), 704-716. doi:10.1109/jproc.2010.2043918.

551 Feddes, R. A., Kowalik, P. J., & Zaradny, H. (1978). Simulation of field water use and crop yield.
552 Centre for Agricultural Publishing and Documentation.

553 Franz, T. E., Wahbi, A., Vreugdenhil, M., Weltin, G., Heng, L., Oismueller, M., et al. (2016).
554 Using cosmic-ray neutron probes to monitor landscape scale soil water content in mixed land
555 use agricultural systems. Applied and Environmental Soil Science, 2016.

556 Franz, T. E., Wang, T., Avery, W., Finkenbiner, C., & Brocca, L. (2015). Combined analysis of
557 soil moisture measurements from roving and fixed cosmic ray neutron probes for multiscale
558 real-time monitoring. Geophysical Research Letters, 42(9), 3389-3396.

559 Franz, T. E., Zreda, M., Ferre, T., Rosolem, R., Zweck, C., Stillman, S., et al. (2012).
560 Measurement depth of the cosmic ray soil moisture probe affected by hydrogen from various
561 sources. Water Resources Research, 48(8).

562 Galleguillos, M., Jacob, F., Prévot, L., Lagacherie, P., & Liang, S. (2011). Mapping daily
563 evapotranspiration over a Mediterranean vineyard watershed. Geoscience and Remote
564 Sensing Letters, IEEE, 8(1), 168-172.

565 Glenn, E. P., Huete, A. R., Nagler, P. L., Hirschboeck, K. K., & Brown, P. (2007). Integrating
566 remote sensing and ground methods to estimate evapotranspiration. Critical Reviews in Plant
567 Sciences, 26(3), 139-168.

568 Guswa, A. J. (2012), Canopy vs. Roots: Production and Destruction of Variability in Soil Moisture
569 and Hydrologic Fluxes, Vadose Zone Journal, 11(3). doi:10.2136/vzj2011.0159.

570 Hawdon, A., McJannet, D., & Wallace, J. (2014). Calibration and correction procedures for
571 cosmic-ray neutron soil moisture probes located across Australia. Water Resources Research,
572 50(6), 5029-5043.

- 573 Hollinger, D. Y., & Richardson, A. D. (2005). Uncertainty in eddy covariance measurements and
574 its application to physiological models. *Tree Physiology*, 25(7), 873-885.
- 575 Hopmans, J.W., Šimunek, J., 1999. Review of inverse estimation of soil hydraulic properties. In:
576 van Genuchten, M.Th. Leij, F.J., Wu, L. (Eds.), *Proceedings of the International Workshop*
577 *Characterization and Measurement of Hydraulic Properties of Unsaturated Porous Media*.
578 University of California, Riverside, 643–659. Irmak, S. (2010). Nebraska water and energy
579 flux measurement, modeling, and research network (NEBFLUX). *Transactions of the*
580 *ASABE*, 53(4), 1097-1115. Irmak, S. (2010). Nebraska water and energy flux measurement,
581 modeling, and research network (NEBFLUX). *Transactions of the ASABE*, 53(4), 1097-1115.
- 582 Izadifar, Z., & Elshorbagy, A. (2010). Prediction of hourly actual evapotranspiration using neural
583 networks, genetic programming, and statistical models. *Hydrological Processes*, 24(23), 3413-
584 3425.
- 585 Jiménez-Martínez, J., Skaggs, T., Van Genuchten, M. T., & Candela, L. (2009). A root zone
586 modelling approach to estimating groundwater recharge from irrigated areas. *Journal of*
587 *Hydrology*, 367(1), 138-149.
- 588 Kalfas, J. L., Xiao, X., Vanegas, D. X., Verma, S. B., & Suyker, A. E. (2011). Modeling gross
589 primary production of irrigated and rain-fed maize using MODIS imagery and CO₂ flux
590 tower data. *Agricultural and Forest Meteorology*, 151(12), 1514-1528.
- 591 Kjaersgaard, J., Allen, R., Trezza, R., Robinson, C., Oliveira, A., Dhungel, R., et al. (2012). Filling
592 satellite image cloud gaps to create complete images of evapotranspiration. *IAHS-AISH*
593 *Publication*, 102-105.
- 594 Köhli, M., Schrön, M., Zreda, M., Schmidt, U., Dietrich, P., & Zacharias, S. (2015). Footprint
595 characteristics revised for field-scale soil moisture monitoring with cosmic-ray neutrons.
596 *Water Resources Research*, 51(7), 5772-5790.

597 Li, Z., Tang, R., Wan, Z., Bi, Y., Zhou, C., Tang, B., et al. (2009). A review of current
598 methodologies for regional evapotranspiration estimation from remotely sensed data. *Sensors*,
599 9(5), 3801-3853.

600 Lv, L., Franz, T. E., Robinson, D. A., & Jones, S. B. (2014). Measured and modeled soil moisture
601 compared with cosmic-ray neutron probe estimates in a mixed forest. *Vadose Zone Journal*,
602 13(12)

603 Maidment, D. R. (1992). *Handbook of hydrology*. McGraw-Hill Inc.

604 Massman, W., & Lee, X. (2002). Eddy covariance flux corrections and uncertainties in long-term
605 studies of carbon and energy exchanges. *Agricultural and Forest Meteorology*, 113(1), 121-
606 144.

607 McMaster, G. S., & Wilhelm, W. (1997). Growing degree-days: One equation, two interpretations.
608 *Agricultural and Forest Meteorology*, 87(4), 291-300.

609 Min, L., Shen, Y., & Pei, H. (2015). Estimating groundwater recharge using deep vadose zone data
610 under typical irrigated cropland in the piedmont region of the north china plain. *Journal of*
611 *Hydrology*, 527, 305-315.

612 Mualem, Y. (1976). A new model for predicting the hydraulic conductivity of unsaturated porous
613 media. *Water Resources Research*, 12(3), 513-522.

614 Nearing, G. S., Mocko, D. M., Peters-Lidard, C. D., Kumar, S. V., & Xia, Y. (2016).
615 Benchmarking NLDAS-2 soil moisture and evapotranspiration to separate uncertainty
616 contributions. *Journal of Hydrometeorology*, 17(3), 745-759.

617 Renzullo, L. J., Van Dijk, A., Perraud, J., Collins, D., Henderson, B., Jin, H., et al. (2014).
618 Continental satellite soil moisture data assimilation improves root-zone moisture analysis for
619 water resources assessment. *Journal of Hydrology*, 519, 2747-2762.

620 Ries, F., Lange, J., Schmidt, S., Puhmann, H., & Sauter, M. (2015). Recharge estimation and soil
621 moisture dynamics in a Mediterranean, semi-arid karst region. *Hydrology and Earth System*
622 *Sciences*, 19(3), 1439-1456.

623 Ritter, A., Hupet, F., Muñoz-Carpena, R., Lambot, S., & Vanclooster, M. (2003). Using inverse
624 methods for estimating soil hydraulic properties from field data as an alternative to direct
625 methods. *Agricultural Water Management*, 59(2), 77-96.

626 Rosolem, R., H. V. Gupta, W. J. Shuttleworth, X. B. Zeng, and L. G. G. de Goncalves (2012), A
627 fully multiple-criteria implementation of the Sobol' method for parameter sensitivity analysis,
628 *J. Geophys. Res.-Atmos.*, 117. doi:10.1029/2011jd016355.

629 Schaap, M. G., Leij, F. J., & Van Genuchten, M. T. (2001). Rosetta: A computer program for
630 estimating soil hydraulic parameters with hierarchical pedotransfer functions. *Journal of*
631 *Hydrology*, 251(3), 163-176.

632 Schymanski, S. J., M. Sivapalan, M. L. Roderick, J. Beringer, and L. B. Hutley (2008), An
633 optimality-based model of the coupled soil moisture and root dynamics, *Hydrology and Earth*
634 *System Sciences*, 12(3), 913-932.

635 Senay, G. B., Budde, M. E., & Verdin, J. P. (2011). Enhancing the simplified surface energy
636 balance (SSEB) approach for estimating landscape ET: Validation with the METRIC model.
637 *Agricultural Water Management*, 98(4), 606-618.

638 Šimunek, J., Šejna, M., Saito, H., Sakai, M., van Genuchten, M.T. (2013). The HYDRUS-1D
639 Software Package for Simulating the One-Dimensional Movement of Water, Heat, and Multiple
640 Solutes in Variably-Saturated Media, Version 4.17. Department of Environmental Sciences,
641 University of California Riverside, Riverside, California, USA, 307 pp.

642 Soil Survey Staff, Natural Resources Conservation Service, United States Department of
643 Agriculture. Web Soil Survey. Available online at <http://websoilsurvey.nrcs.usda.gov/>.
644 Accessed in July, 2016.

- 645 Stoy, P. (2012). Evapotranspiration and energy flux observations from a global tower network with
646 a critical analysis of uncertainties. AGU Fall Meeting Abstracts, 1. pp. 06.
- 647 Suyker, A., Verma, S., Burba, G., Arkebauer, T., Walters, D., & Hubbard, K. (2004). Growing
648 season carbon dioxide exchange in irrigated and rainfed maize. *Agricultural and Forest*
649 *Meteorology*, 124(1), 1-13.
- 650 Suyker, A. E., & Verma, S. B. (2008). Interannual water vapor and energy exchange in an irrigated
651 maize-based agroecosystem. *Agricultural and Forest Meteorology*, 148(3), 417-427.
- 652 Suyker, A. E., & Verma, S. B. (2009). Evapotranspiration of irrigated and rainfed maize–soybean
653 cropping systems. *Agricultural and Forest Meteorology*, 149(3), 443-452.
- 654 Suyker, A. E., Verma, S. B., Burba, G. G., & Arkebauer, T. J. (2005). Gross primary production
655 and ecosystem respiration of irrigated maize and irrigated soybean during a growing season.
656 *Agricultural and Forest Meteorology*, 131(3), 180-190.
- 657 Suyker, A. E., Verma, S. B., Burba, G. G., & Arkebauer, T. J. (2005). Gross primary production
658 and ecosystem respiration of irrigated maize and irrigated soybean during a growing season.
659 *Agricultural and Forest Meteorology*, 131(3), 180-190.
- 660 Turkeltaub, T., Kurtzman, D., Bel, G., & Dahan, O. (2015). Examination of groundwater recharge
661 with a calibrated/validated flow model of the deep vadose zone. *Journal of Hydrology*, 522,
662 618-627.
- 663 Twarakavi, N. K. C., Šimůnek, J., & Seo, S. (2008). Evaluating interactions between groundwater
664 and vadose zone using the HYDRUS-based flow package for MODFLOW. *Vadose Zone*
665 *Journal*, 7(2), 757-768.
- 666 van Genuchten, M. T. (1980). A closed-form equation for predicting the hydraulic conductivity of
667 unsaturated soils. *Soil Science Society of America Journal*, 44(5), 892-898.

668 Verma, S. B., Dobermann, A., Cassman, K. G., Walters, D. T., Knops, J. M., Arkebauer, T. J., et
669 al. (2005). Annual carbon dioxide exchange in irrigated and rainfed maize-based
670 agroecosystems. *Agricultural and Forest Meteorology*, 131(1), 77-96.

671 Wang, T., & Franz, T. E. (2015). Field observations of regional controls of soil hydraulic
672 properties on soil moisture spatial variability in different climate zones. *Vadose Zone Journal*,
673 14(8)

674 Wang, T., Franz, T. E., Yue, W., Szilagyi, J., Zlotnik, V. A., You, J., et al. (2016). Feasibility
675 analysis of using inverse modeling for estimating natural groundwater recharge from a large-
676 scale soil moisture monitoring network. *Journal of Hydrology*, 533, 250-265.

677 Wang, T., Franz, T. E., & Zlotnik, V. A. (2015). Controls of soil hydraulic characteristics on
678 modeling groundwater recharge under different climatic conditions. *Journal of Hydrology*,
679 521, 470-481.

680 Wang, T., Istanbuluoglu, E., Lenters, J., & Scott, D. (2009a). On the role of groundwater and soil
681 texture in the regional water balance: An investigation of the Nebraska sand hills, USA. *Water*
682 *Resources Research*, 45(10)

683 Wang, T., Zlotnik, V. A., Šimunek, J., & Schaap, M. G. (2009b). Using pedotransfer functions in
684 vadose zone models for estimating groundwater recharge in semiarid regions. *Water*
685 *Resources Research*, 45(4)

686 Wolf, A., Saliendra, N., Akshalov, K., Johnson, D. A., & Laca, E. (2008). Effects of different eddy
687 covariance correction schemes on energy balance closure and comparisons with the modified
688 bowen ratio system. *Agricultural and Forest Meteorology*, 148(6), 942-952.

689 Wood, E. F., Roundy, J. K., Troy, T. J., Van Beek, L., Bierkens, M. F., Blyth, E., et al. (2011).
690 Hyperresolution global land surface modeling: Meeting a grand challenge for monitoring
691 earth's terrestrial water. *Water Resources Research*, 47(5)

692 Wösten, J., Pachepsky, Y. A., & Rawls, W. (2001). Pedotransfer functions: Bridging the gap
693 between available basic soil data and missing soil hydraulic characteristics. *Journal of*
694 *Hydrology*, 251(3), 123-150.

695 Xia, Y., Ek, M. B., Wu, Y., Ford, T., & Quiring, S. M. (2015). Comparison of NLDAS-2
696 simulated and NASMD observed daily soil moisture. part I: Comparison and analysis. *Journal*
697 *of Hydrometeorology*, 16(5), 1962-1980.

698 Xie, Y., Sha, Z., & Yu, M. (2008). Remote sensing imagery in vegetation mapping: A review.
699 *Journal of Plant Ecology*, 1(1), 9-23.

700 Yang, H., Dobermann, A., Cassman, K. G., & Walters, D. T. (2004). Hybrid-maize. A Simulation
701 Model for Corn Growth and Yield. Nebraska Cooperative Extension CD, 9.

702 Yang, W., Yang, L., & Merchant, J. (1997). An assessment of AVHRR/NDVI-ecoclimatological
703 relations in Nebraska, USA. *International Journal of Remote Sensing*, 18(10), 2161-2180.

704 Zhang, L., Dawes, W., & Walker, G. (2001). Response of mean annual evapotranspiration to
705 vegetation changes at catchment scale. *Water Resources Research*, 37(3), 701-708.

706 Zhang, Z., Tian, F., Hu, H., & Yang, P. (2014). A comparison of methods for determining field
707 evapotranspiration: Photosynthesis system, sap flow, and eddy covariance. *Hydrology and*
708 *Earth System Sciences*, 18(3), 1053-1072.

709 Zreda, M., Shuttleworth, W., Zeng, X., Zweck, C., Desilets, D., Franz, T., et al. (2012). COSMOS:
710 The cosmic-ray soil moisture observing system. *Hydrology and Earth System Sciences*,
711 16(11), 4079-4099.

712 Zreda, M., Desilets, D., Ferré, T., & Scott, R. L. (2008). Measuring soil moisture content non-
713 invasively at intermediate spatial scale using cosmic-ray neutrons. *Geophysical Research*
714 *Letters*, 35(21).

715

716 **List of Figures**

717 Figure 1. Study site (Mead Rainfed/US-Ne3) location in Nebraska (a) and locations of Eddy-
718 Covariance Tower (EC), Cosmic-Ray Neutron Probe (CRNP), Theta Probes (TPs), and
719 variability of soil texture based on Web Soil Survey data at the study site, 2014 (b). See table 1
720 for soil descriptions.

721 Figure 2. Eddy-Covariance Tower (a) and Cosmic-Ray Neutron Probe (b) Located at the Mead
722 Rainfed (US-Ne3) Site.

723 Figure 3. Daily precipitation (P) and reference evapotranspiration (ET_r) during the calibration
724 (2008–2010) and validation (2011–2012) periods at the Mead Rainfed (US-Ne3) Site.

725 Figure 4. Temporal evolution of daily SWC (θ) at different soil depths. The black lines represent
726 daily mean SWC (θ) calculated from TPs in 4 different locations at study site and the blue areas
727 indicate one standard deviation.

728 Figure 5. Time series of daily CRNP and spatial average TP SWC (θ) data.

729 Figure 6. Annual precipitation (P) and annual actual evapotranspiration (ET_a) at the Mead Rainfed
730 (US-Ne3) Site.

731 Figure 7. Daily observed and simulated SWC (θ) during the calibration (2008–2010) and validation
732 (2011–2012) periods at TP 1 location. See supplemental figures for other comparisons.

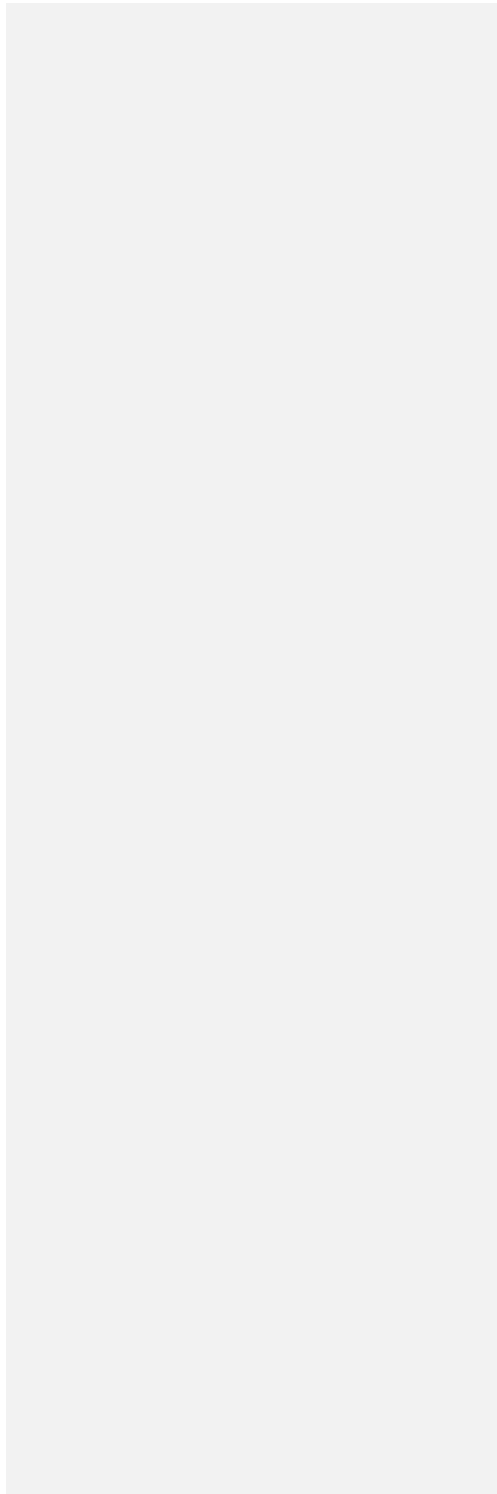
733 Figure 8. Daily observed and simulated SWC (θ) during the calibration (2012–2013) and validation
734 (2014) periods at the location of Cosmic-Ray Neutron probe.

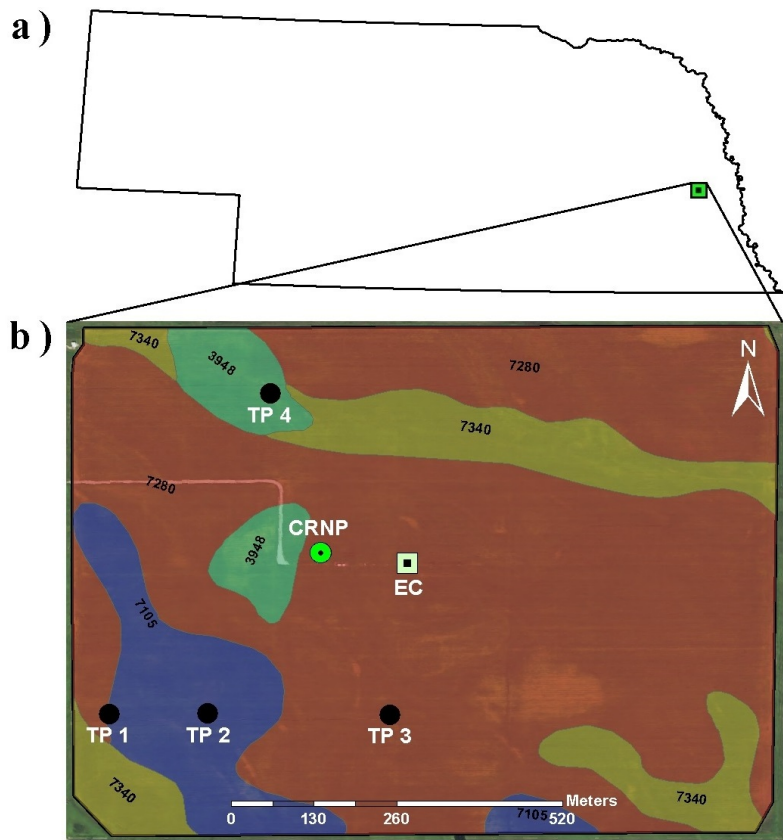
735 Figure 9. Simulated daily ET_a versus Observed daily ET_a in different locations at the study site
736 (2007-2012).

737 Figure 10. Sensitivity Analysis of Effect of Soil Hydraulic Parameters on average annual ET_a
738 values (2007-2012) for a single homogeneous soil layer (6 parameters) and for a 4-layer soil
739 profile (24 parameters).

740 Figure 11. Sensitivity Analysis of Effect of Root Depth on ET_a estimation for a single
741 homogeneous soil layer profile. Note that root depth is in terms of percent depth as it is

742 dynamic over the growing period.





743

744 Figure 1. Study site (Meade Rainfed/US-Ne3) location in Nebraska (a) and locations of Eddy-
 745 Covariance Tower (EC), Cosmic-Ray Neutron Probe (CRNP), Theta Probes (TPs), and
 746 variability of soil texture based on Web Soil Survey data at the study site, 2014 (b). See table 1
 747 for soil descriptions.

748

749

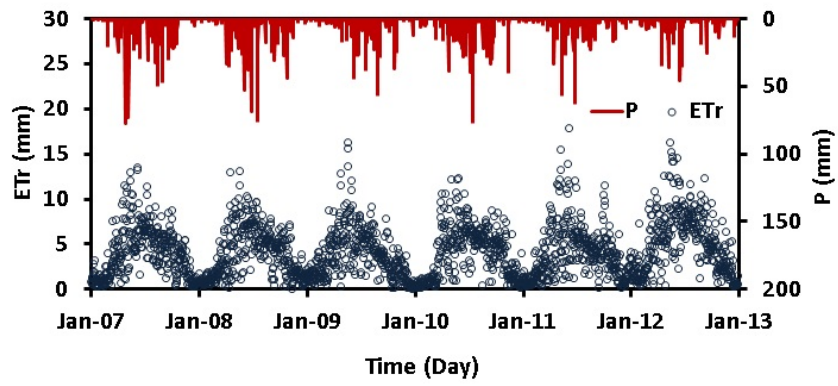


750

751

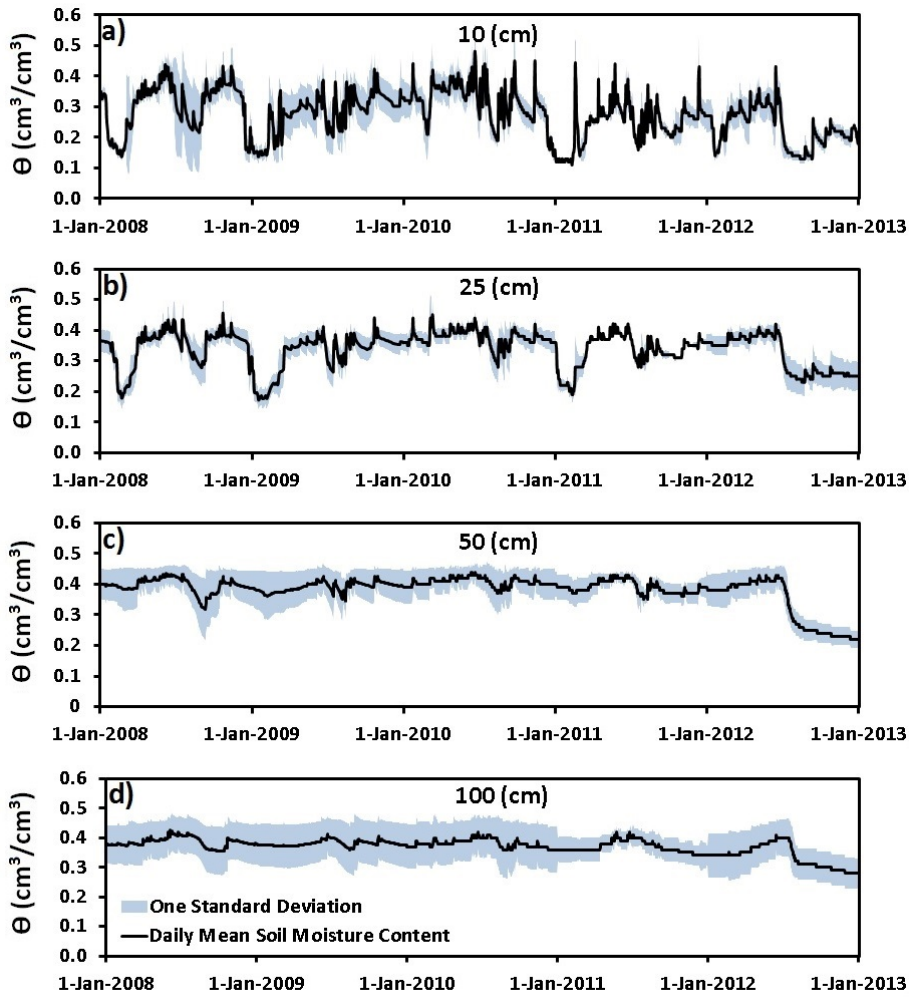
752

Figure 2. Eddy-Covariance Tower (a) and Cosmic-Ray Neutron Probe (b) Located at the Mead Rainfed (US-Ne3) Site.



753
754
755

Figure 3. Daily precipitation (P) and reference evapotranspiration (ET_r) during the calibration (2008–2010) and validation (2011–2012) periods at the Mead Rainfed (US-Ne3) Site.



756

757 Figure 4. Temporal evolution of daily *SWC* (θ) at different soil depths. The black lines represent
 758 daily mean *SWC* (θ) calculated from TPs in 4 different locations at study site and the blue areas
 759 indicate one standard deviation.

760

761

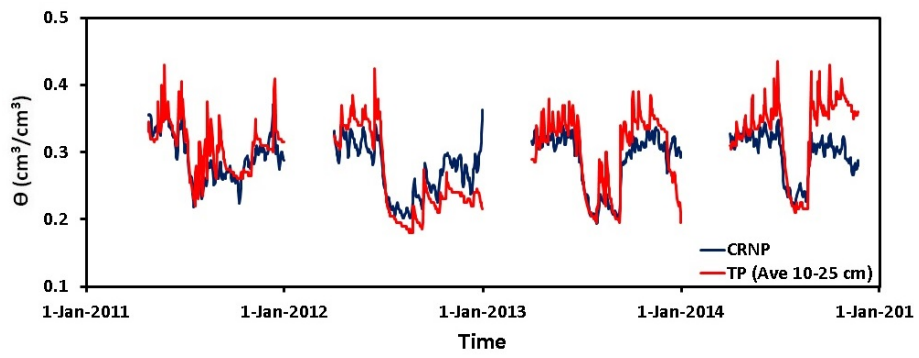
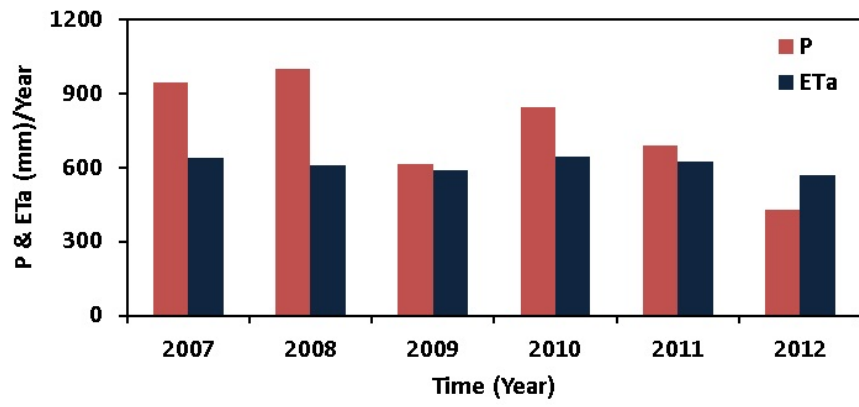


Figure 5. Time series of daily CRNP and spatial average TP *SWC* (θ) data.

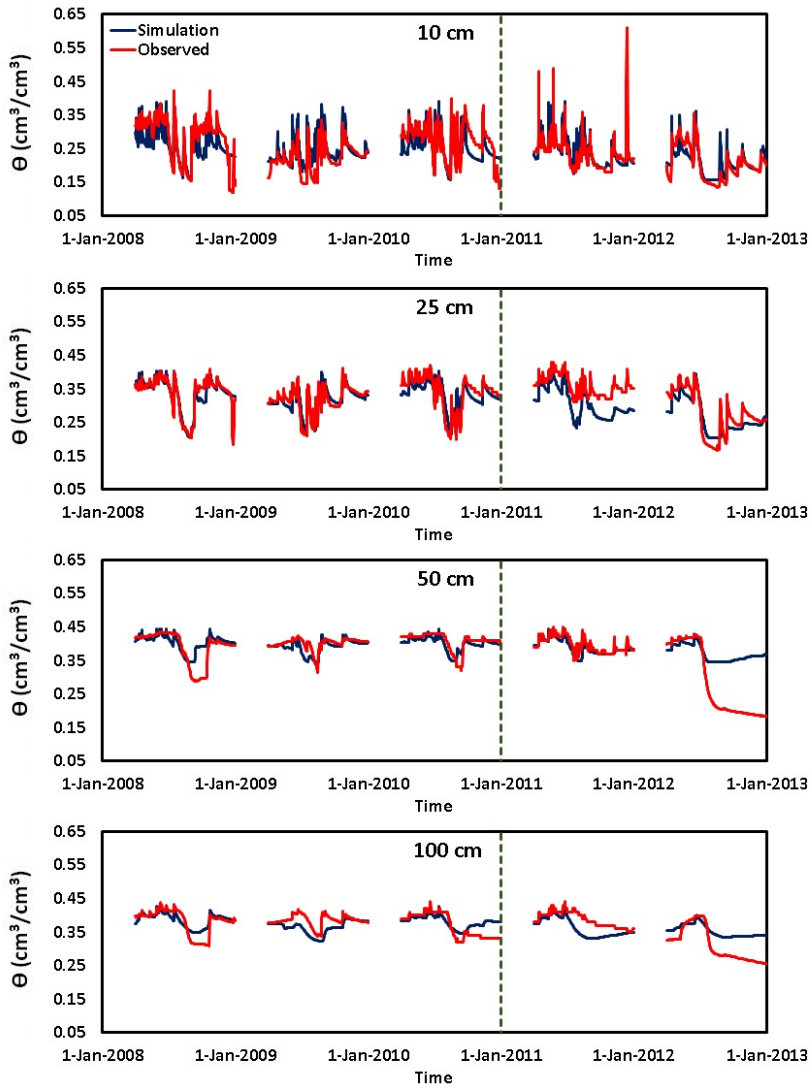
762
 763
 764
 765
 766
 767
 768
 769
 770
 771
 772
 773
 774
 775
 776



777

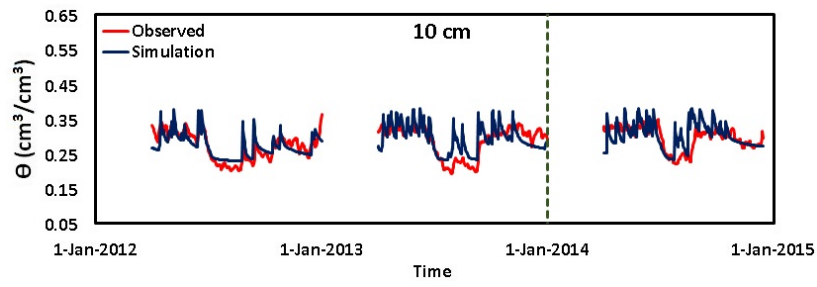
778 Figure 6. Annual precipitation (P) and annual actual evapotranspiration (ET_a) at the Mead Rainfed
 779 (US-Ne3) Site.

780



781

782 Figure 7. Daily observed and simulated *SWC* (θ) during the calibration (2008–2010) and validation
 783 (2011–2012) periods at TP 1 location. See supplemental figures for other comparisons.



784

785 Figure 8. Daily observed and simulated *SWC* (θ) during the calibration (2012–2013) and validation
 786 (2014) periods at the location of Cosmic-Ray Neutron probe.

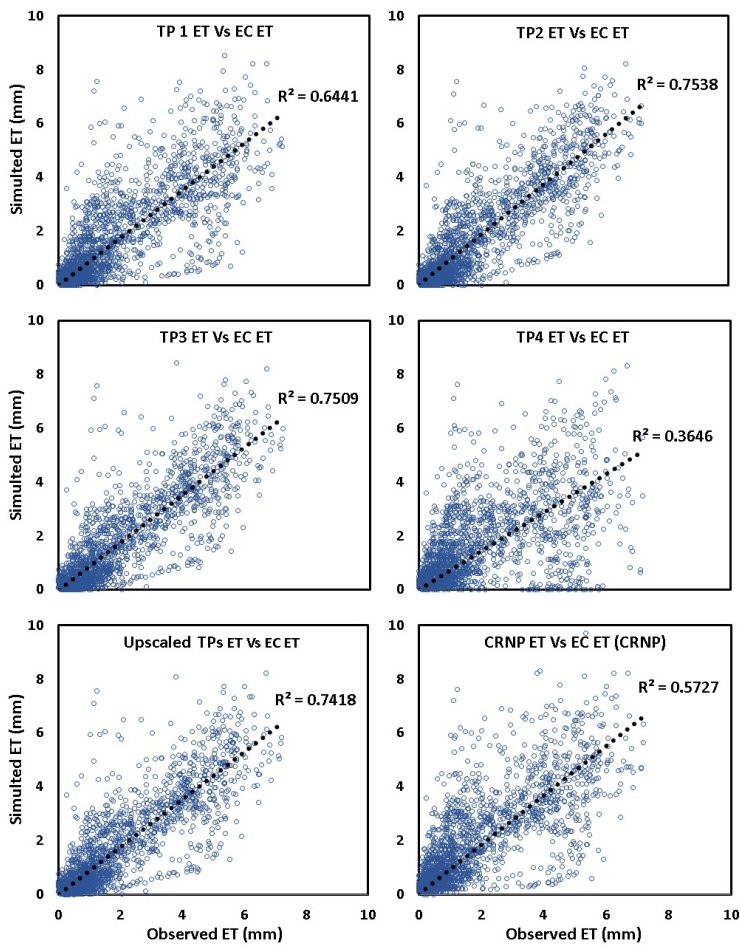
787

788

789

790

791



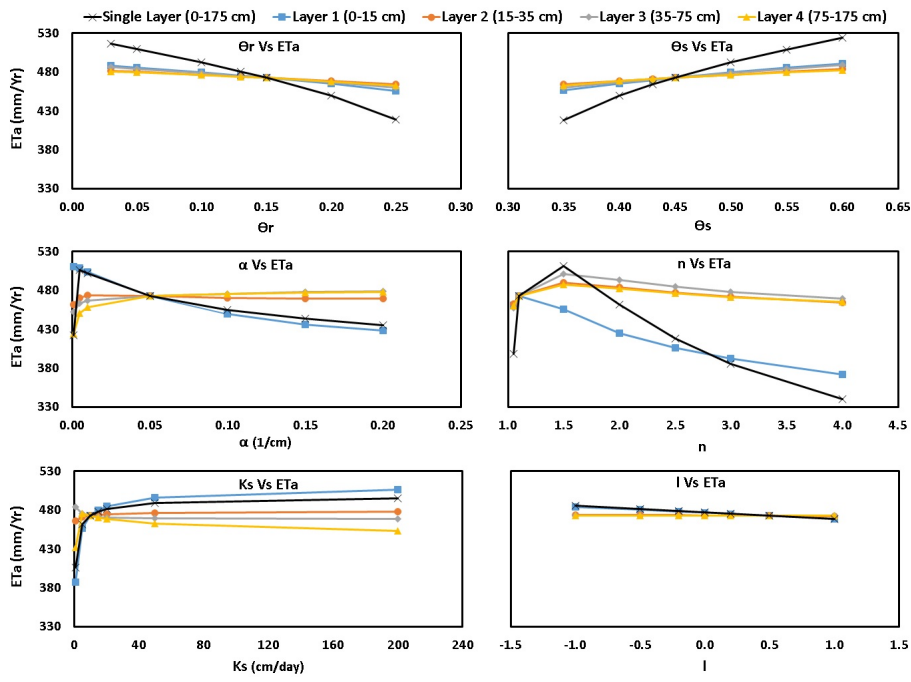
792

793

794

795

Figure 9. Simulated daily ET_a versus observed daily ET_a at different locations in the study site (2007-2012).



796

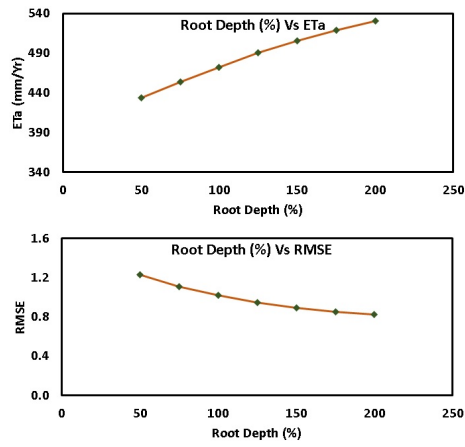
797

798

799

800

Figure 10. Sensitivity analysis of the effect of soil hydraulic parameters on average annual ET_a values (2007-2012) for a single homogeneous soil layer (6 parameters) and for a 4-layer soil profile (24 parameters).



801

802 Figure 11. Sensitivity analysis of root depth on *ETa* estimation for a single homogeneous soil layer
 803 profile. Note that root depth is in terms of percent depth as it is dynamic over the growing period.

804

805

806 **List of Tables**

807 Table 1. Variability of soil texture in the study field based on Web Soil Survey data
808 (<http://websoilsurvey.sc.egov.usda.gov/App/HomePage.htm>).

809 Table 2. Bounds of the van Genuchten parameters used for inverse modeling.

810 Table 3. Goodness-of-fit measures for simulated and observed *SWC* data at different depths during
811 the calibration period (2008 to 2010) and validation period (2011-2012) at TPs locations.

812 Table 4. Goodness-of-fit measures for simulated and observed *SWC* data during the calibration
813 period (2012 to 2013) and validation period (2014) at CRNP location.

814 Table 5. Optimized van Genuchten parameters in different locations at the study site. Note, 95%
815 confidence intervals are in parentheses.

816 Table 6. Goodness-of-fit measures for simulated and observed daily ET_a during the simulation
817 period (2007-2012) at study site.

818 Table 7. Summary of simulated yearly and average actual evapotranspiration (ET_a) (mm) and
819 observed yearly and average actual evapotranspiration (ET_a) (mm) from Eddy-Covariance
820 tower during 2007 to 2012.

821

822

823

824

825

826

827

828
829

Table 1. Variability of soil texture in the study field based on Web Soil Survey data (<http://websoilsurvey.sc.egov.usda.gov/App/HomePage.htm>).

Map Unit Symbol	Map Unit Name	Clay (%)	Silt (%)	Sand (%)	Hectares in Field	Percent of Field
3948	Fillmore silt loam, terrace, occasionally ponded	41.7	51.0	7.3	3.24	4.9%
7105	Yutan silty clay loam, terrace, 2 to 6 percent slopes, eroded	25.8	59.4	14.8	6.88	10.3%
7280	Tomek silt loam, 0 to 2 percent slopes	32.3	61.6	6.1	47.23	70.8%
7340	Filbert silt loam, 0 to 1 percent slopes	41.4	51.7	6.9	9.34	14.0%
Total Area of Field					66.69	100.0%

830

831

832

833

834

835

836

837

838

839

840

Table 2. Bounds of the van Genuchten parameters used for inverse modeling.

Soil Parameter	θ_r (-)	θ_s (-)	α (1/cm)	n (-)	K_s (cm/day)	l (-)
Range	0.03–0.30	0.3–0.6	0.001–0.200	1.01–6.00	1–200	-1–1

841

842

843

844

845

846

847

848

849

850

851

852

853

854

855

856 Table 3. Goodness-of-fit measures for simulated and observed *SWC* data at different depths during
 857 the calibration period (2008 to 2010) and validation period (2011-2012) at TPs locations. Note
 858 we assume a good fit as an RMSE between 0-0.03 cm³/cm³ and fair as between 0.03-0.06
 859 cm³/cm³.

Location	Depth (cm)	Calibration Period (2008-2010)				Validation Period (2011-2012)			
		R ²	MAE (cm ³ /cm ³)	RMSE (cm ³ /cm ³)	NSE	R ²	MAE (cm ³ /cm ³)	RMSE (cm ³ /cm ³)	NSE
TP 1	10	0.542	0.024	0.036	0.533	0.532	0.016	0.033	0.503
	25	0.742	0.014	0.022	0.739	0.716	0.029	0.040	0.486
	50	0.409	0.013	0.023	0.407	0.603	0.041	0.074	0.157
	100	0.352	0.015	0.022	0.343	0.419	0.027	0.038	0.358
TP 2	10	0.330	0.044	0.066	0.305	0.287	0.047	0.061	0.052
	25	0.623	0.010	0.020	0.604	0.718	0.038	0.055	0.135
	50	0.551	0.015	0.026	0.074	0.683	0.040	0.055	0.202
	100	0.424	0.019	0.027	-2.055	0.344	0.048	0.073	-0.473
TP 3	10	0.269	0.034	0.051	0.256	0.534	0.086	0.102	-4.265
	25	0.512	0.011	0.017	0.509	0.852	0.010	0.015	0.793
	50	0.549	0.015	0.023	-0.214	0.658	0.022	0.033	0.652
	100	0.238	0.018	0.029	-3.156	0.669	0.018	0.025	0.178
TP 4	10	0.412	0.029	0.044	0.406	0.580	0.051	0.071	-0.116
	25	0.434	0.016	0.025	0.350	0.594	0.029	0.042	0.490
	50	0.151	0.009	0.015	-13.400	0.443	0.041	0.073	0.036
	100	0.001	0.013	0.021	-12.058	0.292	0.026	0.039	0.238

860

861

862

863

864

865

866 Table 4. Goodness-of-fit measures for simulated and observed *SWC* data during the calibration
867 period (2012 to 2013) and validation period (2014) at CRNP location.

Location	Depth (cm)	Calibration Period (2012-2013)				Validation Period (2014)			
		R ²	MAE (cm ³ /cm ³)	RMSE (cm ³ /cm ³)	NSE	R ²	MAE (cm ³ /cm ³)	RMSE (cm ³ /cm ³)	NSE
CRNP	10	0.497	0.018	0.027	0.456	0.192	0.020	0.032	-0.310

868

869

870

871

872

873

874

875

876

877

878

879

880 Table 5. Optimized van Genuchten parameters in different locations at the study site. Note, 95%
 881 confidence intervals are in parentheses.

Location	Depth (cm)	θ_r (-)	θ_s (-)	α (1/cm)	n (-)	K_s (cm/day)	l (-)
TP 1	0-15	0.134 (0.130-0.137)	0.423 (0.417-0.429)	0.027 (0.026-0.027)	1.475 (1.456-1.494)	8.119 (7.965-8.273)	0.546 (0.525-0.567)
	15-35	0.136 (0.132-0.141)	0.408 (0.404-0.412)	0.007 (0.007-0.007)	1.345 (1.322-1.367)	11.540 (11.137-11.939)	0.480 (0.466-0.494)
	35-75	0.191 (0.188-0.194)	0.448 (0.443-0.453)	0.024 (0.024-0.025)	1.097 (1.088-1.105)	8.057 (7.879-8.235)	0.285 (0.278-0.292)
	75-175	0.071 (0.068-0.073)	0.430 (0.424-0.436)	0.025 (0.024-0.025)	1.069 (1.061-1.077)	9.807 (9.540-10.073)	0.364 (0.354-0.375)
TP 2	0-15	0.211 (0.195-0.227)	0.446 (0.431-0.461)	0.027 (0.018-0.035)	1.567 (1.431-1.703)	8.120 (4.660-11.580)	1.000 (0.411-1.589)
	15-35	0.197 (0.105-0.289)	0.434 (0.425-0.442)	0.006 (0.003-0.008)	1.191 (1.076-1.306)	8.655 (0.953-16.357)	0.022 (-0.194-0.238)
	35-75	0.110 (0-0.258)	0.424 (0.406-0.441)	0.015 (0.007-0.023)	1.239 (1.040-1.438)	4.605 (0-9.214)	0.723 (-1.210-2.655)
	75-175	0.109 (0-0.275)	0.408 (0.357-0.459)	0.020 (0-0.044)	1.302 (0.965-1.639)	6.780 (0-20.523)	0.000 (-0.045-0.045)
TP 3	0-15	0.281 (0.276-0.287)	0.464 (0.463-0.465)	0.035 (0.033-0.036)	1.487 (1.446-1.528)	7.096 (6.742-7.450)	0.400 (0.385-0.416)
	15-35	0.072 (0.069-0.075)	0.402 (0.398-0.407)	0.012 (0.011-0.012)	1.085 (1.076-1.095)	29.960 (28.470-31.457)	0.353 (0.340-0.367)
	35-75	0.081 (0.076-0.087)	0.498 (0.481-0.515)	0.037 (0.034-0.039)	1.128 (1.108-1.149)	24.440 (22.013-26.872)	0.527 (0.472-0.583)
	75-175	0.085 (0.077-0.092)	0.500 (0.482-0.518)	0.039 (0.036-0.042)	1.147 (1.124-1.170)	17.540 (15.995-19.088)	0.496 (0.454-0.539)
TP 4	0-15	0.082 (0.069-0.096)	0.481 (0.474-0.489)	0.034 (0.030-0.038)	1.172 (1.158-1.186)	7.773 (6.913-8.632)	0.953 (0.772-1.133)
	15-35	0.200 (0.175-0.225)	0.426 (0.420-0.433)	0.013 (0.010-0.017)	1.217 (1.173-1.262)	14.060 (9.248-18.873)	0.044 (0.027-0.061)
	35-75	0.250 (0.240-0.260)	0.477 (0.472-0.481)	0.009 (0.007-0.011)	1.079 (1.066-1.092)	1.045 (0.952-1.138)	0.353 (0.168-0.538)
	75-175	0.200 (0.185-0.214)	0.487 (0.481-0.494)	0.012 (0.009-0.014)	1.070 (1.057-1.083)	1.454 (1.146-1.762)	0.985 (0.706-1.264)
CRNP	0-15	0.100 (0.098-0.103)	0.392 (0.386-0.398)	0.019 (0.018-0.019)	1.054 (1.145-1.164)	6.931 (6.786-7.076)	0.547 (0.545-0.549)

882

883
884

Table 6. Goodness-of-fit measures for simulated and observed daily ET_a during the simulation period (2007-2012) at study site.

Location	R ²	MAE (mm/day)	RMSE (mm/day)	NSE
ET_a	0.510	1.359	1.992	0.340
TP 1	0.644	0.696	1.062	0.618
TP 2	0.754	0.610	0.907	0.746
TP 3	0.751	0.601	0.904	0.728
TP 4	0.365	0.878	1.387	0.168
TPs Weighted Average	0.742	0.599	0.911	0.714
CRNP	0.573	0.742	1.143	0.562

Formatted: Subscript

885
886
887
888
889
890
891
892
893
894
895
896

897

898
899
900

Table 7. Summary of simulated yearly and average actual evapotranspiration (ET_a) (mm) and observed yearly and average actual evapotranspiration (ET_o) (mm) from Eddy-Covariance tower during 2007 to 2012.

Location	Year						
	2007	2008	2009	2010	2011	2012	Average
ET_p	1048.5	987.9	989.4	1011.5	1025.7	1326.7	1064.9
EC	656.8	608.4	589.7	646.1	622.2	570.1	612.5
TP 1	646.1	629.0	559.8	642.1	573.9	415.5	579.5
TP 2	614.3	598.4	576.7	620.5	576.9	429.5	574.7
TP 3	529.0	556.1	556.4	590.4	549.8	405.2	545.4
TP 4	652.2	576.1	529.9	677.3	458.2	381.2	525.3
Upscaled TPs	613.9	564.1	556.3	600.3	547.7	405.9	548.0
CRNP	745.3	707.1	603.0	721.8	642.2	439.3	643.1

Formatted: Subscript

901